CNWRA 94-023
(Revision 1)

A THREE-DIMENSIONAL GEOLOGICAL FRAMEWORK MODEL FOR YUCCA MOUNTAIN, NEVADA, WITH HYDROLOGIC APPLICATION: REPORT TO ACCOMPANY 1995 MODEL TRANSFER TO THE NUCLEAR REGULATORY COMMISSION

Prepared for

Nuclear Regulatory Commission
Contract NRC-02-93-005

Prepared by

Center for Nuclear Waste Regulatory Analyses
San Antonio, Texas

September 1995

CNWRA 94-023
(Revision 1)

A THREE-DIMENSIONAL GEOLOGICAL FRAMEWORK MODEL FOR YUCCA MOUNTAIN, NEVADA, WITH HYDROLOGIC APPLICATION: REPORT TO ACCOMPANY 1995 MODEL TRANSFER TO THE NUCLEAR REGULATORY COMMISSION

Prepared for

Nuclear Regulatory Commission
Contract NRC-02-93-005

Prepared by

Gerry L. Stirewalt
D. Brent Henderson

Center for Nuclear Waste Regulatory Analyses
San Antonio, Texas

September 1995

PREVIOUS REPORTS IN SERIES

Number	Name	Date Issued
CNWRA 94-023	A Preliminary Three-Dimensional Geological Framework Model for Yucca Mountain, Nevada: Report to Accompany Model Transfer to the Nuclear Regulatory Commission	September 1994

ABSTRACT

The updated three-dimensional (3D) geological framework model and preliminary hydrostratigraphic model applications described in this report were developed for the potential high-level radioactive waste disposal site at Yucca Mountain, Nevada, by staff at the Center for Nuclear Waste Regulatory Analyses. The models were constructed for the Nuclear Regulatory Commission (NRC) using EarthVision software (Versions 2.0 and 2.9 beta) from Dynamic Graphics, Inc. of Alameda, California.

The 3D geological framework model is comprised of eight lithostratigraphic units and includes, from east to west across the model volume, the Bow Ridge, Ghost Dance, and Solitario Canyon fault zones. The 3D model provides the basic volume within which variations in geological features both in and adjacent to the potential repository block can be displayed and visually analyzed and from which two-dimensional (2D) cross sections can be produced for use in 2D computational analyses. The 3D model also provides the geological framework within which alternative tectonic concepts can be considered and submodels constructed by incorporating specific data into the framework model. The two preliminary hydrostratigraphic models described are examples of "submodel" development applications of the 3D geological framework model. These two models separately incorporate porosity and saturated hydraulic conductivity data into the geological framework model for illustrating variations in these hydrologic properties within the eight lithostratigraphic units represented. The geological framework model will be refined and modified, and additional submodels for representing hydrologic and other properties of the lithostratigraphic units constructed, as new data become available.

The 3D geological framework model and submodels like those represented by the preliminary hydrostratigraphic model applications can be used by the NRC during both pre-licensing and licensing phases to assess if the geologic and hydrologic characteristics of models generated by the U.S. Department of Energy (DOE) and its contractors, for use in analysis of site suitability and repository design and performance, are supported by field data and are reasonable. From all models, 2D cross sections can also be extracted for use in calculations and analyses. It is feasible that the 3D framework model and submodels can be applied to focus on Key Technical Issues (KTIs) related to structural deformation and seismicity, hydrologic characterization of structural features, and the exploratory studies facility (ESF). These three KTIs are among those that the NRC deem necessary for the DOE to resolve for preparation of an acceptable license application.

CONTENTS

CONTENTS (Cont'd)

FIGURES

TABLES

ACKNOWLEDGMENTS

This report was prepared to document work performed by the Center for Nuclear Waste Regulatory Analyses (CNWRA) for the Nuclear Regulatory Commission (NRC) under Contract No. NRC-02-93-005. The activities reported here were performed on behalf of the NRC Office of Nuclear Material Safety and Safeguards (NMSS), Division of Waste Management (DWM). The report is an independent product of the CNWRA and does not necessarily reflect the views or regulatory position of the NRC.

The authors wish to thank J. Stamatakos and R. Baca for their valuable technical reviews of this report, B. Sagar for careful programmatic review, and B. Mabrito for verification of compliance with Quality Assurance Procedure 002 (QAP-002). The authors also appreciate the able and timely assistance of B. Long, E. Cantú, and Southwest Research Institute Publications Services who assured an on-schedule submittal of the report. G. Rice compiled and summarized data used in the hydrostratigraphic models for elevation of the water table and porosities and saturated hydraulic conductivities of the eight lithostratigrahic units comprising the models. He also reviewed Section 4 on hydrostratigraphic model applications. S. Young and J. Bangs constructed the earliest versions of the 3D model using EarthVision software. A. Morris was instrumental in preparing balanced cross sections used to provide subsurface control in the model. R. Martin provided invaluable geographic information systems (GIS) database support. R. Klar and H. Castellaw digitized input data and C. Fenrich implemented several significant improvements in the current updated three-dimensional (3D) geological framework model. The authors appreciate the assistance of all these individuals.

QUALITY OF DATA, ANALYSES, AND CODE DEVELOPMENT

DATA: Data used to construct the foundation 3D geological framework model in which hydrologic parameters (i.e., porosity and saturated hydraulic conductivity) were included to produce the preliminary 3D hydrostratigraphic models were taken from the published sources referenced in this report. Basic field data on lithology, stratigraphy, and structure were taken from Scott and Bonk (1984). Balanced geological cross sections developed from the data of Scott and Bonk (1984) by CNWRA staff (Young et al., 1992) were used to constrain depths of the eight lithostratigraphic horizons in the 3D model in combination with data from eight boreholes located in the lines of the cross sections. The boreholes were drilled during U.S. Department of Energy (DOE) field investigations of the Yucca Mountain site for acquisition of data on subsurface lithologies and groundwater hydrology. Specific information on porosity and saturated hydraulic conductivity of the eight lithostratigraphic units comprising the model and elevation of the water table for the model area was acquired from borehole descriptions provided in U.S. Geological Survey (USGS) open-file and water resources investigations reports (Anderson, 1981, 1992; Rush et al., 1983; Lahoud et al., 1984; Whitfield et al., 1985; Craig and Reed, 1989; Flint and Flint, 1990). While the data acquired by Scott and Bonk (1984) and from some of the drilling activities were not collected under formal QA programs, use of standard methods for drilling, collection of field and borehole data, testing of samples, and analyses of geological and hydrological information indicates that the data are appropriate for construction of preliminary 3D geological framework and hydrostratigraphic models. The DOE may qualify some of the existing data, or additional data may be collected in accordance with a formal Quality Assurance program. The CNWRA 3D geological framework model will be updated when such data become available. No CNWRA-generated original data are contained in this report. Sources for other data should be consulted for determining the level of quality for those data.

ANALYSES AND CODES: EarthVision software (Versions 2.0 and 2.9 beta) from Dynamic Graphics, Inc. of Alameda, California (Dynamic Graphics, Inc., 1994a and 1994b) was used to prepare appropriate data files and construct the 3D geological framework and hydrostratigraphic models. This commercially available software was purchased from DGI by the CNWRA and is not controlled under the CNWRA Software Configuration Procedures. GEOSEC software (Version 2.0) from CogniSeis Development, Inc. of Houston, Texas (CogniSeis Development, Inc., 1991) was employed to prepare the three balanced geological cross sections which provided subsurface information for use in construction of the 3D model. This commercially available software is accessible through a consultant to CNWRA, Dr. Alan P. Morris of the University of Texas at San Antonio, and is not controlled under the CNWRA Software Configuration Procedures. No code development was undertaken for this report.

1 INTRODUCTION

The updated three-dimensional (3D) geological framework model of the potential high-level radioactive waste (HLW) disposal site at Yucca Mountain described in this report is the current version of the model being developed for the Nuclear Regulatory Commission (NRC) by staff of the Geology and Geophysics (GLGP) Program Element at the Center for Nuclear Waste Regulatory Analyses (CNWRA). The first version of the model, presented to the NRC in September 1994 (Stirewalt et al., 1994), was an extension of the work initiated by Young et al. (1992) on construction of 3D structural and stratigraphic models. The preliminary 3D hydrostratigraphic models, also described in this report, comprise the initial models constructed by incorporating information on porosity and saturated hydraulic conductivity for each of eight lithologic units represented in the 3D geological framework model. The hydrostratigraphic models may be thought of as "submodels" that represent an application of the geological framework model for illustrating variations in the selected hydrologic parameters at Yucca Mountain. Because the geological framework model is based on available data from Scott and Bonk (1984) and on geological interpretations of those data as represented in balanced cross sections (Young et al., 1992), the model is as geologically realistic as the incorporated data allow. Hydrologic data on porosity and saturated hydraulic conductivity of the eight lithostratigraphic units comprising the model, drawn from U.S. Geological Survey (USGS) open-file and water resources investigations reports on descriptions of specific boreholes (Anderson, 1981 and 1992; Rush et al., 1983; Lahoud et al., 1984; Whitfield et al., 1985; Craig and Reed, 1989; Flint and Flint, 1990), are from boreholes concentrated mainly in the east-central part of the model.

EarthVision software (Versions 2.0 and 2.9 beta) from Dynamic Graphics, Inc. of Alameda, California (Dynamic Graphics, Inc., 1994a and b), was used at the CNWRA to prepare data files and construct the geologic framework and hydrostratigraphic models being supplied to the NRC on 4-mm tape with this descriptive report. Silicon Graphics, Inc. hardware is employed at the CNWRA for using EarthVision to construct and view the 3D geological framework and hydrostratigraphic models. EarthVision software is also in place in the NRC computer center at the NRC offices, Two White Flint North (TWFN), Rockville, Maryland, and compatible hardware exists there for examining the models and their associated databases. Therefore, transfer of the models on tape will make it possible for NRC staff to view them at TWFN. The file size for each 3D model is about 14 Mb. In addition to the 3D models, which are being relayed on tape as faces files with this report, script and data files are also being provided. Appendix A lists all files being transferred to the NRC with the 3D models.

Submission to the NRC of the updated 3D geological framework and preliminary hydrostratigraphic models and supporting script and data files, along with this descriptive report, satisfy the Intermediate Milestone deliverable for the NRC Office of Nuclear Material Safety and Safeguards Task 20-5702-425-507. The prime responsibility for this task lies with the GLGP Program Element at the CNWRA, although the hydrostratigraphic models discussed in Section 4 were developed for the CNWRA Performance Assessment (PA) Program Element under Task 20-5702-723. With submittal of the report, the models, and the supporting files, the initial 3D geological framework model submitted to the NRC in September 1994 (Stirewalt et al., 1994) is superseded and becomes archival information. The report is not a manual describing the detailed use of EarthVision software for 3D model construction, but rather a concise description of the geological framework and hydrostratigraphic models developed using the software.

2 PURPOSE OF THE THREE-DIMENSIONAL GEOLOGICAL FRAMEWORK MODEL

The 3D geological framework model can be used by NRC staff during both prelicensing and licensing activities to assess geological models of Yucca Mountain chosen by the Department of Energy (DOE) for use in analyses of site suitability, design, and repository performance. Key Technical Uncertainties (KTUs) related to development and use of conceptual tectonic models are defined in the License Application Review Plan (LARP) of the NRC (Nuclear Regulatory Commission, 1994), specifically in review plans 3.2.1.5 and 3.2.1.9. These KTUs make it important for NRC staff to be able to consider models provided by the DOE in light of how realistically these models represent subsurface geological features. The KTUs are at the level for which the LARP (Nuclear Regulatory Commission, 1994) requires detailed safety review supported by independent tests and analyses. Therefore, the NRC staff will need an independently developed model to compare with conceptual models proposed by the DOE for determining whether representation of subsurface geological features and conditions in the DOE models are reasonable and adequate.

3 DESCRIPTION OF THE THREE-DIMENSIONAL GEOLOGICAL FRAMEWORK MODEL

As specified in the report on the initial version of the 3D geological framework model (Stirewalt et al., 1994), development of the model was to be iterative in the sense that it was to be modified as additional data became available. Consequently, this updated version of the framework model has been developed at the CNWRA as planned. Just as for earlier versions of the model (Stirewalt et al., 1994; Stirewalt and Henderson, 1995), the updated version also provides the geological framework in which variations in geological features in and adjacent to the repository block can be illustrated and analyzed, submodels can be constructed, and alternative models can be considered. Model boundaries, topography, boreholes used for subsurfaces control on lithostratigraphic units and faults, and faults included are the same as for the initial version (Stirewalt et al., 1994). Specific changes in the updated model are indicated in Section 3.2. The first submodel applications, preliminary hydrostratigraphic models developed by including hydrologic parameters (i.e., porosity and saturated hydraulic conductivity) in the geological framework model, are described in Section 4.

Boundaries of the 3D geological framework model, types and sources of data used in model development and construction, model construction approach, and characteristics of the model are discussed in Section 3. The steps followed for construction of the 3D geological framework model, discussed in Sections 3.1 and 3.2 and summarized in the flow chart of Figure 3-1, are as follows:

- Establish boundaries for the 3D model volume (Section 3.1).

- Create balanced geological cross sections to provide subsurface control on lithostratigraphy and faults (Sections 3.2.2 and 3.2.4). Use borehole data (Section 3.2.3) to provide additional subsurface control.

- Digitize and plot stratigraphic unit elevations and positions of faults from balanced geological cross sections (Sections 3.2.2 and 3.2.4).

- Interpret extensions of stratigraphic horizons and fault surfaces away from the cross sections and borehole control points by constructing hand-drawn structural contour maps, and digitize stratigraphic horizon and fault elevation data from these maps (Sections 3.2.2 and 3.2.4).

- Use the EarthVision two-dimensional (2D) Minimum Tension Gridding tool (Dynamic Graphics, Inc., 1994a) to construct gridded 3D surfaces representing topography (Section 3.2.1), tops of lithostratigraphic horizons (Section 3.2.2), fault surfaces (Section 3.2.4), and the water table (Section 3.2.5).

- Apply the EarthVision Geologic Structure Builder (GSB) tool (Dynamic Graphics, Inc., 1994b) to construct the 3D volume model from gridded 3D surfaces representing topography, tops of lithostratigraphic horizons, fault surfaces, and the water table.

- Drape imagery data over the surface of the 3D volume model (Section 3.2.6) using the EarthVision Faces Merge tool (Dynamic Graphics, Inc., 1994a).

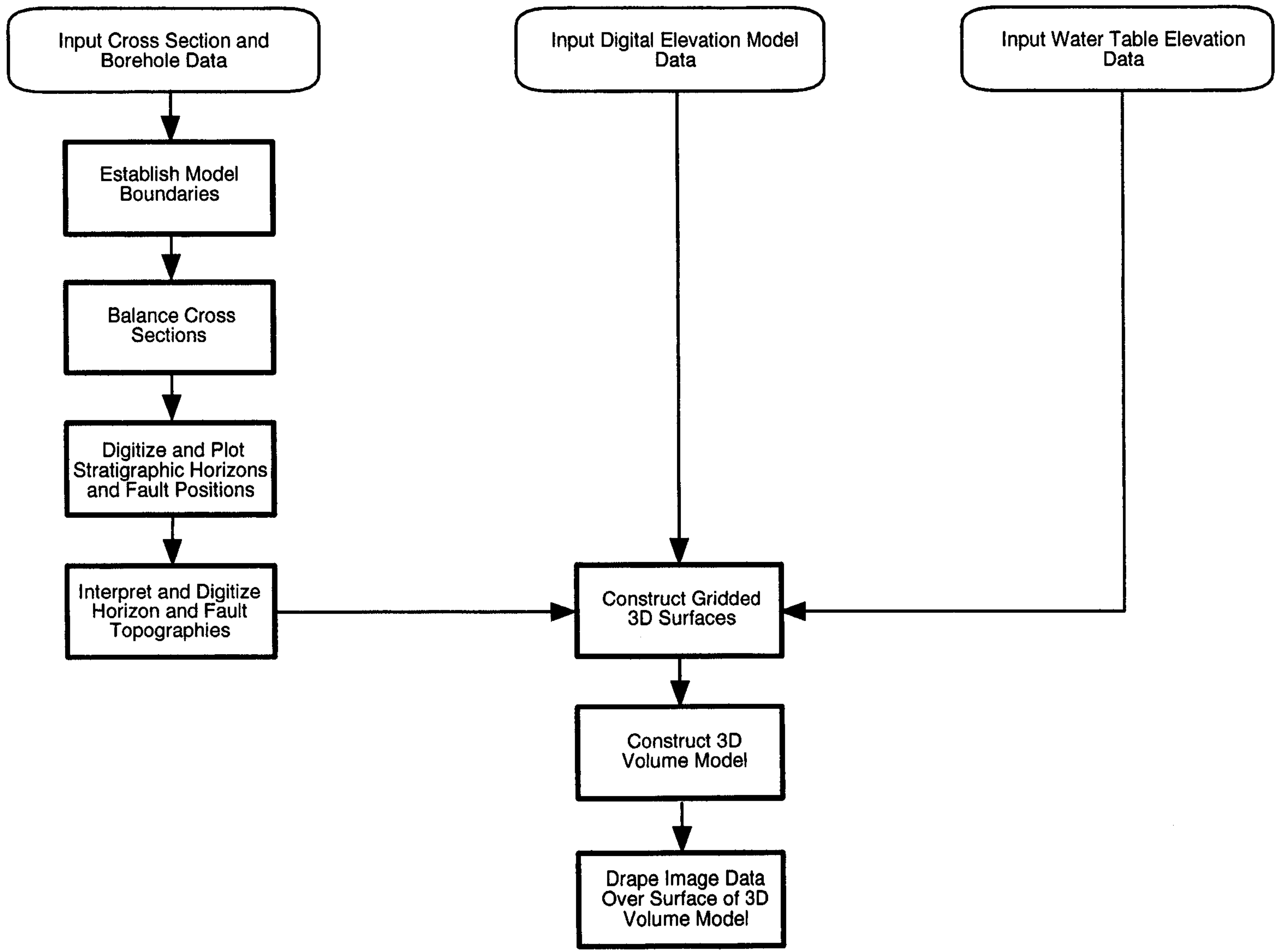

Figure 3–1. Flow diagram illustrating successive steps in construction of the 3D geological framework model

3.1 MODEL BOUNDARIES

Surface boundaries of the 3D geological framework model encompass the potential repository block and three major faults (Section 3.2.4) in and adjacent to the block. The boundaries, illustrated in Figure 3-2, extend north-south out to about 5-km from the repository block and east-west from Midway Valley to West Ridge. Therefore, the lateral dimensions of the model volume are approximately 9 km in a north-south direction and 6 km east-west. Figure 3-2 also shows locations of the three geological cross sections (Section 3.2.2) and eight boreholes (Section 3.2.3) which provided subsurface control on fault surfaces (Section 3.2.4) and depths and thicknesses of the eight lithostratigraphic units (Section 3.2.2) in the 3D model, as well as locations of boreholes from which water table elevations (Section 3.2.5) were taken. Table 3-1 provides information that locates the corners of the 3D geological model boundaries in terms of Nevada State Plane (NSP) and Universal Transverse Mercator (UTM) coordinates, as well as longitude and latitude, for ease of comparison with boundaries of other models. In the vertical dimension, the model volume extends from an elevation of 1800 m above sea level (to include the highest point on Yucca Mountain at an elevation of 1752 m) down to sea level (to pass below the bottom contact of the Bullfrog Member of the Crater Flat Tuff at 350 m above sea level). The EarthVision GSB tool (Dynamic Graphics, Inc., 1994b) was used to incorporate the boundaries into the 3D volume model.

3.2 DATA, MODELING APPROACH, AND MODEL CHARACTERISTICS

Changes in the updated 3D model include the following additions and modifications: (i) two lithostratigraphic units below the welded Prow Pass member of the Crater Flat Tuff (PPw) were added (Section 3.2.2), specifically, nonwelded undifferentiated Upper Crater Flat Tuff (CFUn) and the welded Bullfrog Member of the Crater Flat Tuff (BFw); (ii) the water table was added (Section 3.2.5); (iii) surface distribution of the uppermost lithostratigraphic unit, the Tiva Canyon Formation (Tpcw), was modified so that intersections of the modeled subsurface units with the ground surface of the 3D model more closely represent the outcrop pattern of the units as observed in the field; (iv) intersections of lithostratigraphic units with fault surfaces were modified so that the units properly terminate against faults; (v) Landsat 5 Thematic Mapper (TM) and aerial photographic imagery data were added as draped overlay images (Section 3.2.6); and (vi) hangingwall or footwall blocks can now be selectively removed along a fault to permit viewing of the fault surface (Section 3.2.4). The updated model was constructed using data from the sources indicated throughout this section. Characteristics of the model can be expected to change further as new data become available and are incorporated into the model. Figure 3-3 illustrates the current version of the 3D geological framework model relative to representation of topography, lithostratigraphy, faults, and the water table.

3.2.1 Topography

Information on surface topography was provided from USGS digital elevation data in Digital Elevation Model (DEM) format. These data are a standard source for representing surface topography and have a 30-m pixel resolution at Yucca Mountain. The EarthVision 2D Minimum Tension Gridding tool (Dynamic Graphics, Inc., 1994a) was employed to develop a gridded 3D surface from the DEM data for representing topography in the framework model. The EarthVision GSB tool (Dynamic Graphics, Inc., 1994b) was used to build the 3D volume model from the gridded 3D surfaces representing topography and the other model elements (i.e., tops of lithostratigraphic horizons, fault surfaces, and the water table).

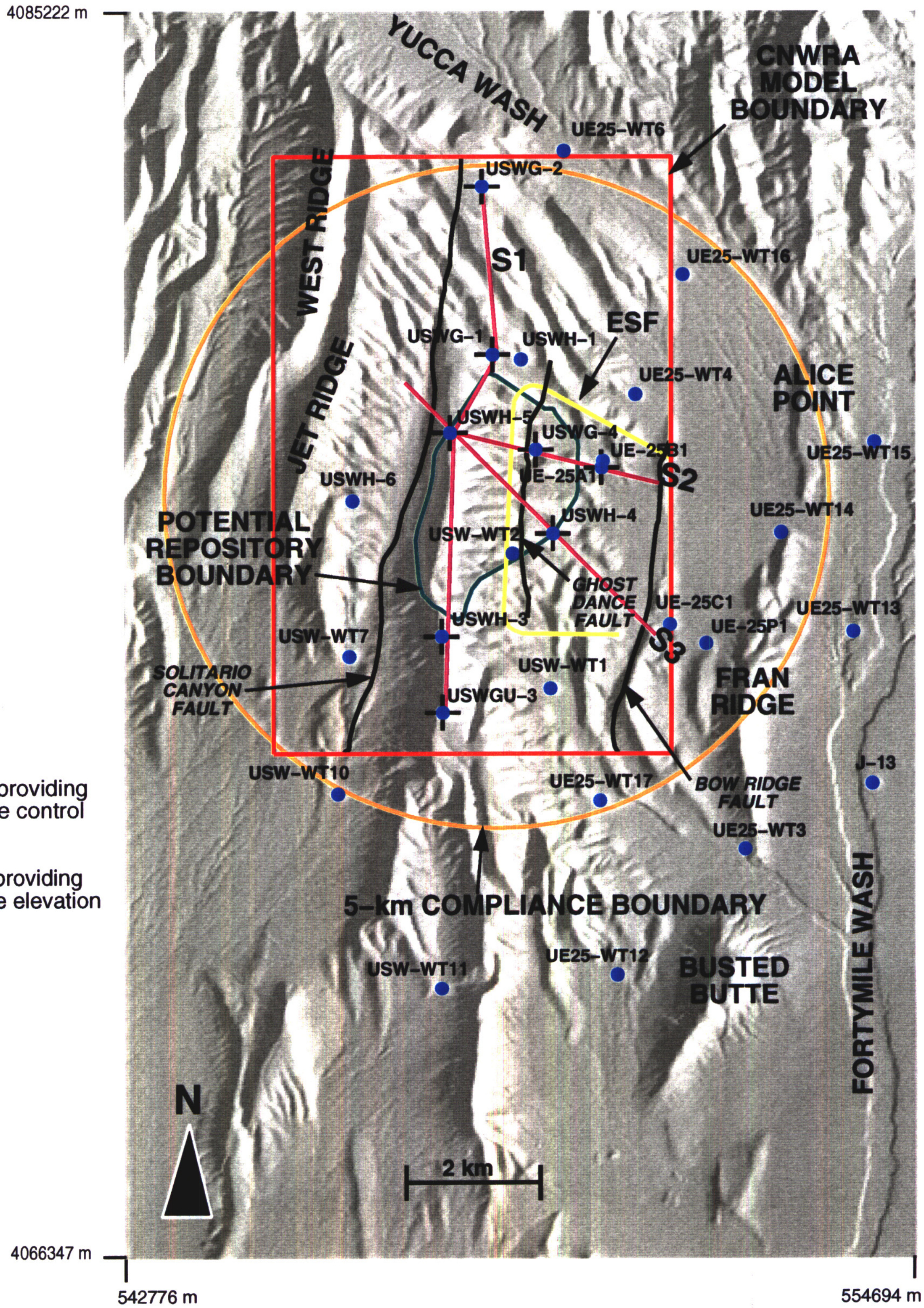

+ Borehole providing subsurface control data

● Borehole providing water table elevation data

Figure 3–2. Boundaries of the CNWRA 3D geological framework model for Yucca Mountain; locations of cross sections (S1, S2, S3) and boreholes providing subsurface control on stratigraphic units and faults; and locations of boreholes containing water table elevation data. Universal Transverse Mercator (UTM) coordinates are indicated.

Table 3-1. Corners of the 3D geological framework model boundaries expressed as Nevada State Plane (NSP) and Universal Transverse Mercator (UTM) coordinates and longitude/latitude

NSP Zn#2702 (ft)	NSP Zn#2702 (ft)	UTM Zn#11 Easting (m)	UTM Zn#11 Northing (m)	Longitude (deg)	Latitude (deg)
550138.97E	750788.51N	545010	4074000	116.50W	36.81N
550242.03E	780324.03N	545010	4083000	116.49W	36.89N
569730.83E	750720.21N	550980	4074000	116.43W	36.81N
569833.89E	780255.61N	550980	4083000	116.43W	36.89N

3.2.2 Lithology and Stratigraphy

The 3D geological framework model consists of a collection of stacked surfaces representing the top contacts of eight lithostratigraphic units. Two additional units have been incorporated since the model was first submitted to the NRC (Stirewalt et al., 1994). The top contact surfaces were initially defined by extracting elevation data for the surfaces from eight boreholes (Section 3.2.3), located in the lines of three balanced geological cross sections produced by Young et al. (1992) from cross sections originally constructed by Scott and Bonk (1984), and the balanced cross sections themselves. Locations of the sections and boreholes that provided data on depths to lithostratigraphic contacts and thicknesses of units are shown in Figure 3-2. Elevation data for tops of the lithostratigraphic horizons extracted from the balanced sections and boreholes were sparse. Consequently, for extending contacts of lithostratigraphic units out from the boreholes and balanced cross sections, structural contour maps were constructed for the top of each horizon using the extracted elevation data as control points. These maps were digitized directly, stored in electronic data files, and stacked in the 3D model to represent the top contacts of the individual lithostratigraphic units. This approach for extending the surfaces provided geological control where data were sparse, rather than permitting the EarthVision software algorithm to construct the positions of unit contacts between control points.

The geological cross sections were balanced using GEOSEC (Version 2.0) software from CogniSeis Development, Inc. of Houston, Texas (CogniSeis Development, Inc., 1991), which operates to generate balanced sections by maintaining areas represented in the original cross sections. Balanced, area-true cross sections were used in construction of the 3D model because they are considered to present internally consistent, geologically reasonable but non-unique, two-dimensional (2D) interpretations of the subsurface geological framework (Dahlstrom, 1969; Woodward et al., 1989; Young et al., 1991). The sections are balanced in the sense that subsurface geometric and kinematic relationships between fault shape and deformation features in hangingwall blocks of faults are represented in a geologically reasonable manner. Hence, balanced sections provide a basis for input of geologically realistic and reasonable subsurface information into the 3D model. Data from additional boreholes, the Exploratory Studies Facility (ESF), and field mapping studies will provide information on lithologic and stratigraphic relationships which can be incorporated into later iterations of the 3D model for refining elevations of contacts and thicknesses of lithostratigraphic units and unit descriptions.

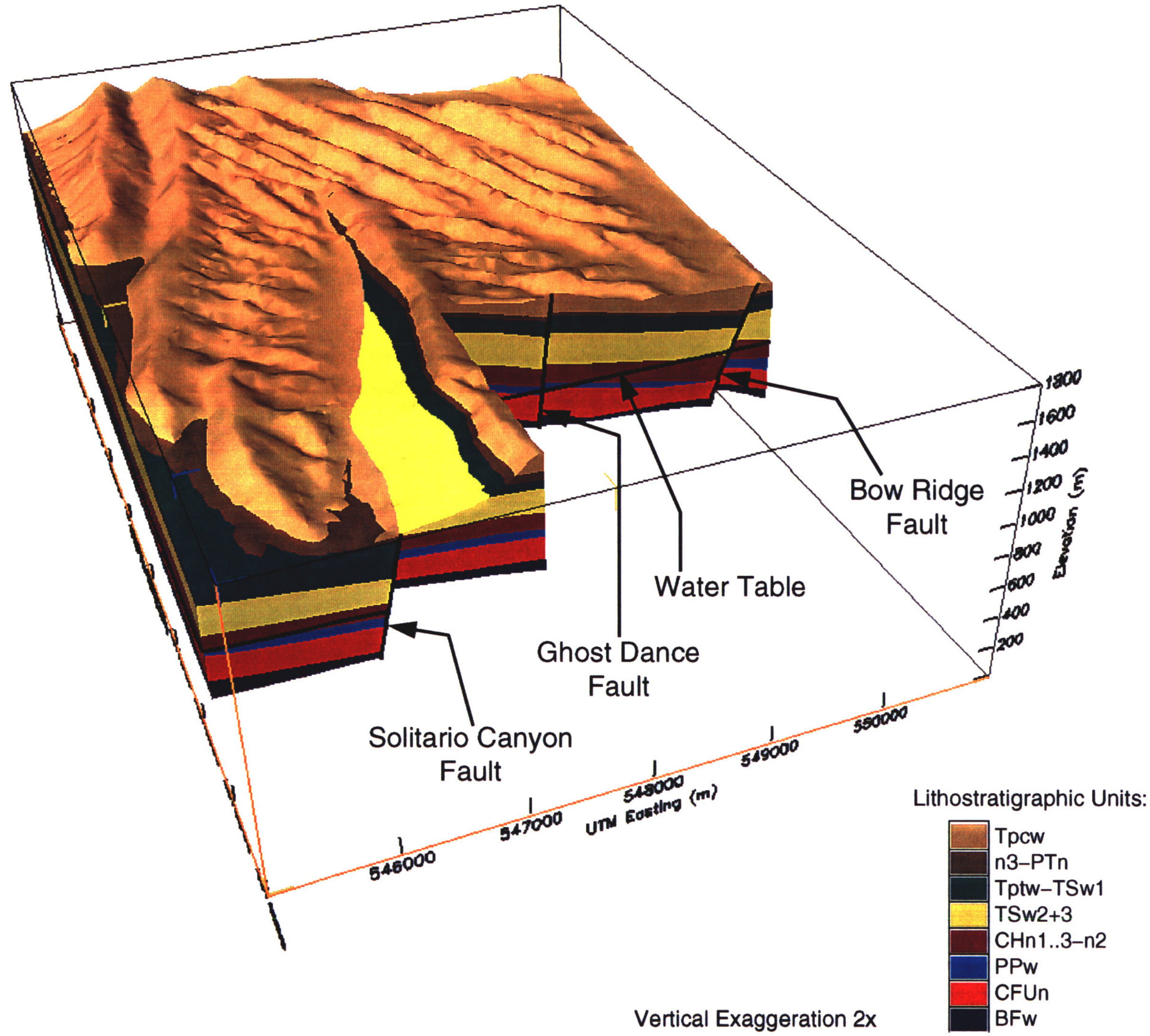

Figure 3–3. Lithostratigraphic units and faults included in the CNWRA 3D geological framework model for Yucca Mountain. The model was constructed using EarthVision software (versions 2.0 and 2.9 beta) from Dynamic Graphics, Inc. (1994a and 1994b). See text (Section 3.2.2) for lithologic descriptions of the lithostratigraphic units.

From youngest to oldest, the lithostratigraphic units in the 3D model (Figure 3-3) include the eight Tertiary volcanic units listed in Table 3-2. Lithostratigraphic unit designations were derived by combining nomenclature used by Ortiz et al. (1985) for their reference stratigraphy with that from Scott and Bonk (1984) for their lithostratigraphy. The reference stratigraphy nomenclature of Ortiz et al. (1985) was established to broadly indicate thermal, mechanical, hydrological, and physical properties of the lithostratigraphic units. After the terminology of Scott and Bonk (1984), the letter "w" in a unit designation indicates that unit is generally classified as moderately to densely welded, while "n" commonly delineates a non-welded to partially welded unit.

Lithostratigraphic descriptions for the 3D model were taken from Scott and Bonk (1984) and Ortiz et al. (1985). The Tiva Canyon and Topopah Spring units, formerly classified by Scott and Bonk (1984) as members of the Paintbrush Tuff Formation, are in the process of being formally reclassified as formations of the newly designated Paintbrush Tuff Group by the USGS (Dickerson and Spengler, 1994) based on more detailed investigation of the lithostratigraphic units. Hence, the names shown for these two units of the Paintbrush Tuff reflect the progress of the USGS in starting to formally reclassify the Paintbrush Tuff from a formation to a group with subsequent upgrading of former members to formations (Dickerson and Spengler, 1994).

The EarthVision 2D Minimum Tension Gridding tool (Dynamic Graphics, Inc., 1994a) was employed to develop gridded 3D surfaces for representing the top contacts of the lithostratigraphic horizons in the geological framework model. The EarthVision GSB tool (Dynamic Graphics, Inc., 1994b) was applied to build the 3D volume model from the gridded 3D surfaces representing tops of lithostratigraphic horizons and the other model elements (i.e., topography, fault surfaces, and the water table).

3.2.3 Borehole Data

Data from eight boreholes, contained in the lines of the three original geological cross sections of Scott and Bonk (1984) which were balanced by Young et al. (1992), provided information for constraining depths to and thicknesses of lithostratigraphic units in the 3D geological framework model. This information was incorporated into the 3D model through use of the balanced cross sections of Young et al. (1992) for construction of the model. The specific boreholes that provided the data included UE-25a1, USWG-4, USWH-5, USWG-1, USWG-2, USWH-3, USWGU-3, and USWH-4. Locations of these boreholes are shown in Figure 3-2. The boreholes were drilled during various phases of DOE field investigations at Yucca Mountain for characterizing subsurface lithologies and groundwater hydrology.

3.2.4 Faults and Fault Zones

From east to west, faults included in the updated model are the northeasterly-striking Bow Ridge, Ghost Dance, and Solitario Canyon faults. Locations of the surface traces of these faults are illustrated in Figure 3-2, and they are represented in the current version of the 3D model as dip-slip (normal) faults (Figure 3-3). The northeasterly-trending Fatigue Wash and Windy Wash faults, located west of the Solitario Canyon fault in the northwestern part of the model volume, and the northwest-striking Sundance fault, located in the repository block near the northern extent of the Ghost Dance fault (Spengler et al., 1994), are not yet included in the model, but will be incorporated in later iterations.

Table 3-2. Lithostratigraphic units included in the 3D geological framework model

Lithostratigraphic Unit Designation	Lithostratigraphic Unit Name and Description
Tpcw	Tiva Canyon Formation of the Paintbrush Tuff Group (moderately to densely welded ashflow tuffs)
n3-PTn	Undifferentiated Formations of the Upper Paintbrush Tuff, including the Lower Tiva Canyon, Yucca Mountain, Pah Canyon, and Topopah Spring units (non-welded to partially welded tuffs)
Tptw-TSw1	Topopah Spring Formation of the Paintbrush Tuff Group (lithophysae-rich, moderately to densely welded ashflow tuffs)
TSw2+3	Topopah Spring Formation of the Paintbrush Tuff Group (proposed repository horizon comprised of lithophysae-poor, moderately to densely welded ashflow tuffs with basal vitrophyre)
Chn1..3-n2	Undifferentiated Calico Hills, Lower Paintbrush Tuff, and Upper Crater Flat Tuff (zeolitic, non-welded ashflow tuffs with bedded tuffs)
PPw	Prow Pass Member of the Crater Flat Tuff (moderately welded ashflow tuffs)
CFUn	Undifferentiated Upper Crater Flat Tuff, including the Lower Prow Pass and Upper Bullfrog units (zeolitic, non-welded to partially welded ashflow tuffs and bedded tuffs)
BFw	Bullfrog Member of the Crater Flat Tuff (moderately to densely welded ashflow tuffs)

Basic information included in the model on fault location, dip, and displacement was derived from Scott and Bonk (1984). Information from balanced geological cross sections (Young et al., 1992) was used to constrain subsurface fault geometry as well as thicknesses of offset lithostratigraphic units. Although faults were modeled as listric features at depths below the model volume in balanced cross sections developed by Young et al. (1991 and 1992), these structures are represented as planar dip-slip (normal) fault surfaces in the 3D model since listric characteristics of the faults were not exhibited in the balanced sections at a depth comparable to that of the model volume. Fault surfaces were projected downward across the lithostratigraphic units for representing the faults at depth. In the balanced cross sections, intersections of fault surfaces with each unit (i.e., "fault cutoffs") were positioned at depth using data from the sections. Away from the balanced sections, fault cutoffs were positioned by projecting the ground-surface trace of the fault downward through each unit using the dip angle of the fault surface as determined from the balanced cross sections. Locations of intersections of the three major faults with the tops of the lithostratigraphic units away from the balanced sections were included on the structural contour maps drawn for representing the unit surfaces between boreholes and cross sections (Section 3.2.2). These fault positions (i.e., fault elevation data) were digitized directly from the structural contour maps and stored in electronic data files. When the data were extracted from the electronic files and the lithostratigraphic units stacked to construct the solid 3D model volume, individual fault cutoffs were checked and aligned as necessary to define positions of the fault surfaces at depth with due consideration for representing a reasonable subsurface geometry for the fault surfaces as dictated by fault dip measurements in surface exposures. This approach for extending the fault surfaces at depth provided a geological basis for the extension where data were sparse rather than permitting the software algorithm to automatically compute the positions of the fault surfaces between control points lying in the cross sections. Detailed mapping of structures in the repository block (Spengler et al., 1993 and 1994; Buesch et al., 1994) may provide additional information on faulting which will be incorporated into later iterations of the model. The Fatigue Wash, Windy Wash, and other faults also will be included as deemed pertinent. Detailed mapping of fault zones in the repository block should provide additional information that can be incorporated into the 3D model.

The EarthVision 2D Minimum Tension Gridding tool (Dynamic Graphics, Inc., 1994a) was employed to develop gridded 3D surfaces for representing the faults in the geological framework model. The EarthVision GSB tool (Dynamic Graphics, Inc., 1994b) was applied to compute the 3D volume model from the gridded 3D surfaces representing faults and the other model elements (i.e., topography, tops of lithostratigraphic horizons, and the water table). As an improvement related to representation of faults, hangingwall and footwall blocks of the faults have been modeled as distinct elements of the 3D volume and can be selectively removed along a fault to permit viewing of the fault surface. Figure 3-4 illustrates the capability of EarthVision software to strip away a fault block for examining the fault surface in the 3D model.

3.2.5 Water Table

Elevation data used for defining the water table in the 3D model were derived from the 28 boreholes listed in Table 3-3 based on information provided by Robison (1984) and Fridrich et.al. (1994). Locations of these boreholes are shown in Figure 3.2. The EarthVision 2D Minimum Tension Gridding tool (Dynamic Graphics, Inc., 1994a) was employed to develop a gridded 3D surface from water table elevation data for representing the water table in the geological framework model. The EarthVision GSB tool (Dynamic Graphics, Inc., 1994b) was applied to compute the 3D volume model from the gridded 3D surfaces representing the water table and the other model elements (i.e., topography, tops of lithostratigraphic horizons, and fault surfaces). As an additional refinement, the water table was represented as a fault surface in the 3D model to allow the model volume above or below the water table to be removed using the EarthVision 3D Viewer tool (Dynamic Graphics, Inc., 1994a). Figure 3-5 illustrates removal of the model volume above the water table to permit viewing of the units lying below the water table.

3.2.6 Draped Imagery

It is possible to use EarthVision software for superimposing images over the surface of the 3D model. Two examples of imagery draped over the model were constructed to illustrate this capability. One example was created using a composite image generated from the red, green, and blue bands of a Landsat 5 TM data set for the Yucca Mountain region (Figure 3-6). This TM data set, dated May 7, 1990, was collected with the sun illumination positioned at an azimuth of 117° and an elevation of 57°.

The second was produced with an aerial photographic image of the Yucca Mountain region superimposed over the surface of the 3D model (Figure 3-7). Date and sun illumination position were unknown for this image. Both types of imagery were draped over the model surface and carefully registered to topography using the EarthVision Faces Merge tool (Dynamic Graphics, Inc., 1994a).

Superimposing on the surface of the model cultural features such as buildings, roads, and rail lines related to development of the repository facility is an obvious application of this capability. Any other natural and cultural features which can be captured by remotely sensed or photographic images could also be superimposed. In the case of repository surface facility features, it would be possible to visually analyze locations of these features relative to each other or to natural elements of the site once the images were draped over the model surface.

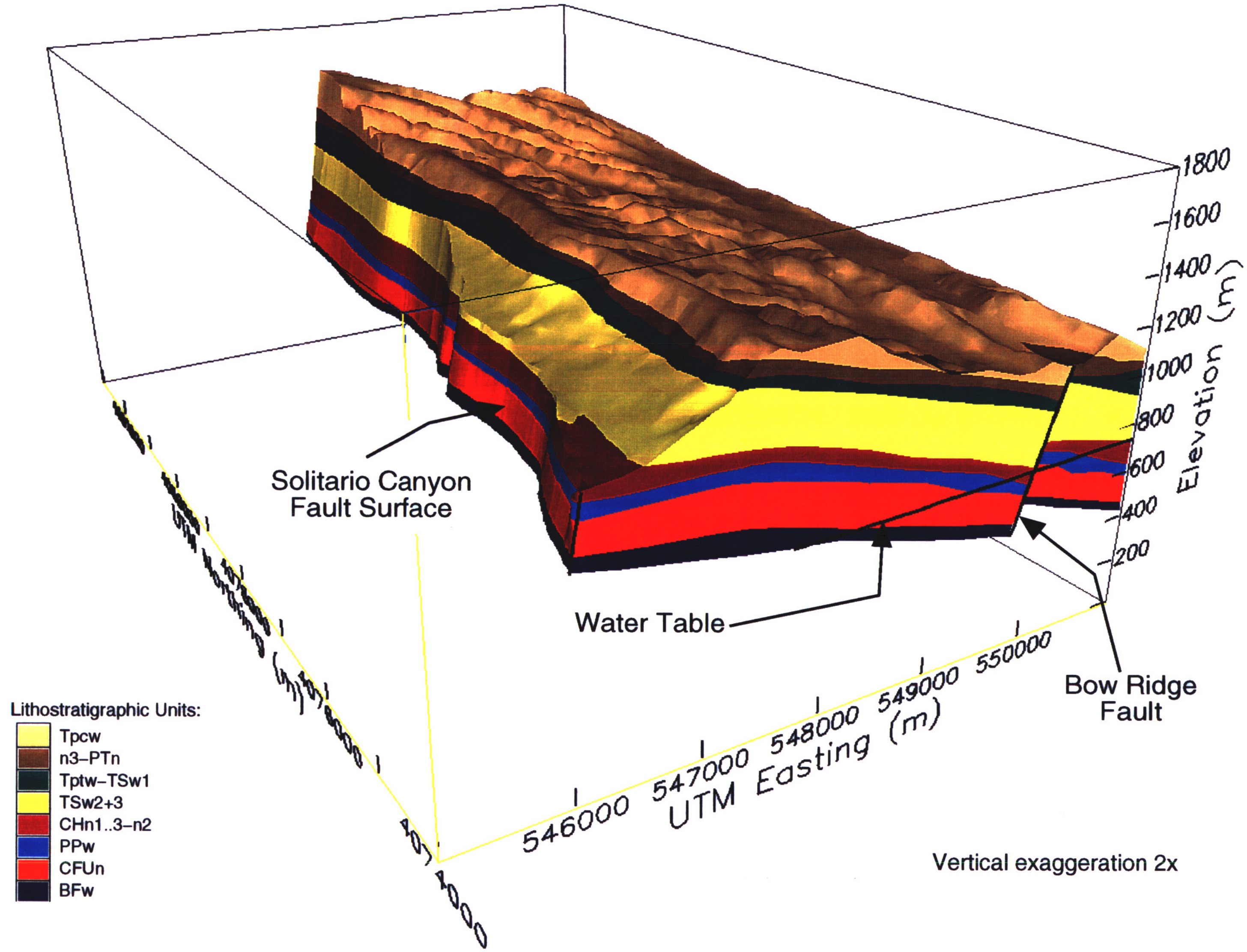

Figure 3–4. Perspective view of the CNWRA 3D geological framework model with the hangingwall block of the Solitario Canyon fault removed to expose the fault surface bounding the footwall block

Table 3-3. Boreholes from which water table elevations were derived for the 3D geological framework model in meters above sea level (masl)

Well ID Number	Water Level (masl)	Ground Surface Elevation (masl)	E UTM (m)	N UTM (m)
UE-25 A-1	730.4	1199.2	549934.74	4078317.21
UE-25 B-1	730.4	1200.7	549954.49	4078421.79
UE-25 C-1	730.1	1130.6	550957.74	4075942.75
UE-25 P-1	730.1	1114.2	551508.73	4075662.80
UE-25 WT-3	729.5	1030.0	552098.20	4072564.04
UE-25 WT-4	730.4	1169.2	550445.87	4079419.63
UE-25 WT-6	1035.0	1314.8	549361.65	4083091.98
UE-25 WT-12	729.5	1074.7	550162.90	4070647.01
UE-25 WT-13	729.2	1032.5	553724.05	4075836.30
UE-25 WT-14	730.2	1075.9	552637.97	4077336.61
UE-25 WT-15	729.0	1083.2	554033.70	4078702.35
UE-25 WT-16	738.2	1210.9	551157.19	4081222.40
UE-25 WT-17	729.6	1124.0	549910.20	4073295.35
USW G-1	753.8	1325.5	548298.56	4080017.92
USW G-2	1029.0	1553.9	548138.26	4082554.14
USW G-3	730.2	1480.6	547550.43	4074615.70
USW G-4	730.1	1269.6	548937.97	4078590.11
USW H-1	730.7	1303.0	548721.77	4079944.44
USW H-3	732.4	1483.3	547536.99	4075762.00
USW H-4	730.1	1248.5	549195.00	4077322.46
USW H-5	775.1	1478.9	547665.51	4078837.67
USW H-6	775.6	1301.7	546196.07	4077816.31
J-13	728.3	1011.3	554004.44	4073550.05
USW WT-1	730.1	1201.4	549150.78	4074975.06
USW WT-2	730.3	1301.3	548590.58	4077020.81
USW WT-7	775.7	1196.9	546148.22	4075460.98
USW WT-10	775.7	1123.4	545975.96	4073388.60
USW WT-11	730.2	1094.1	547532.69	4070437.95

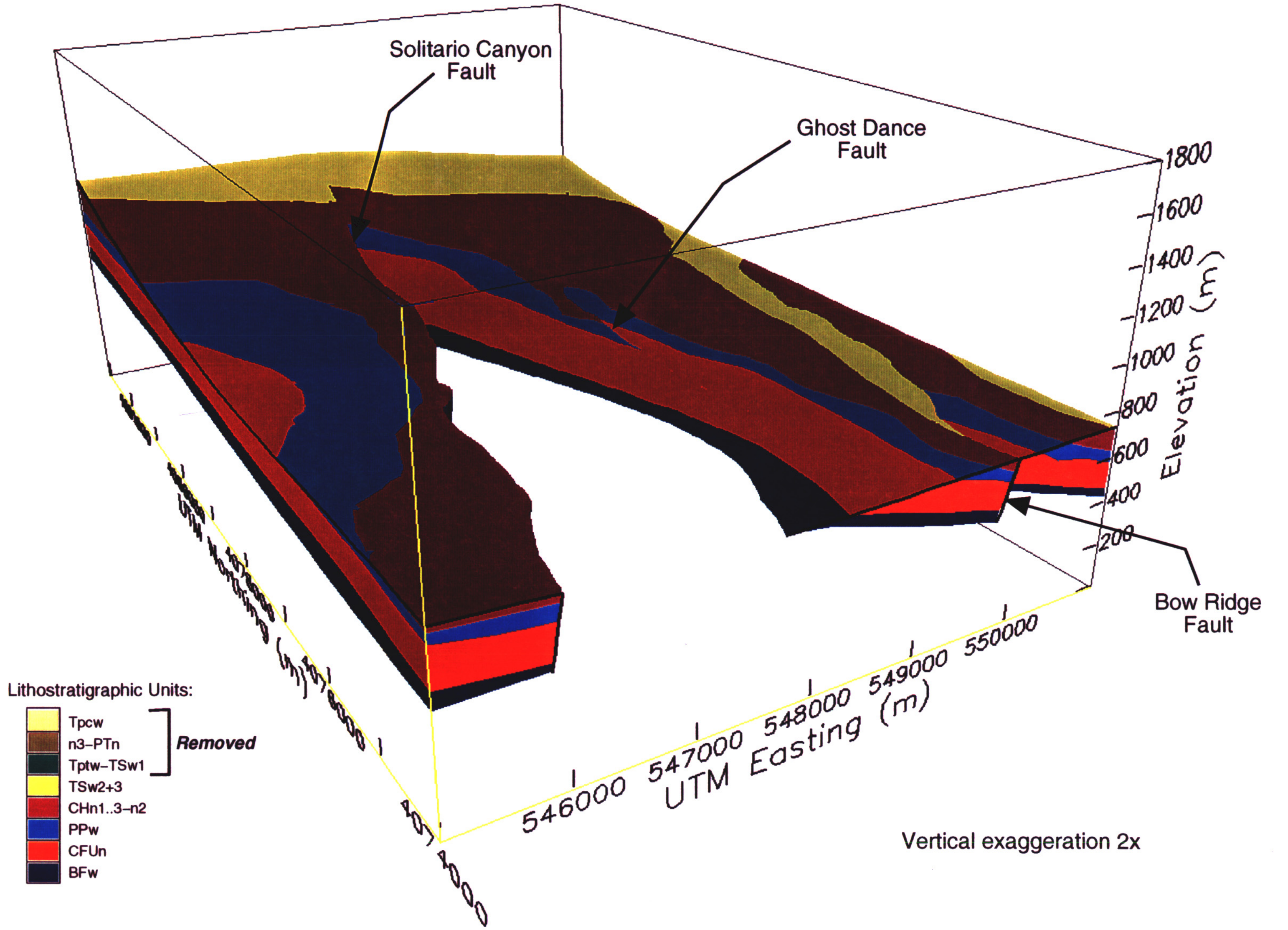

Figure 3–5. Perspective view of the CNWRA 3D geological framework model with portions of lithostratigraphic units above the water table surface removed to expose units lying below the water table

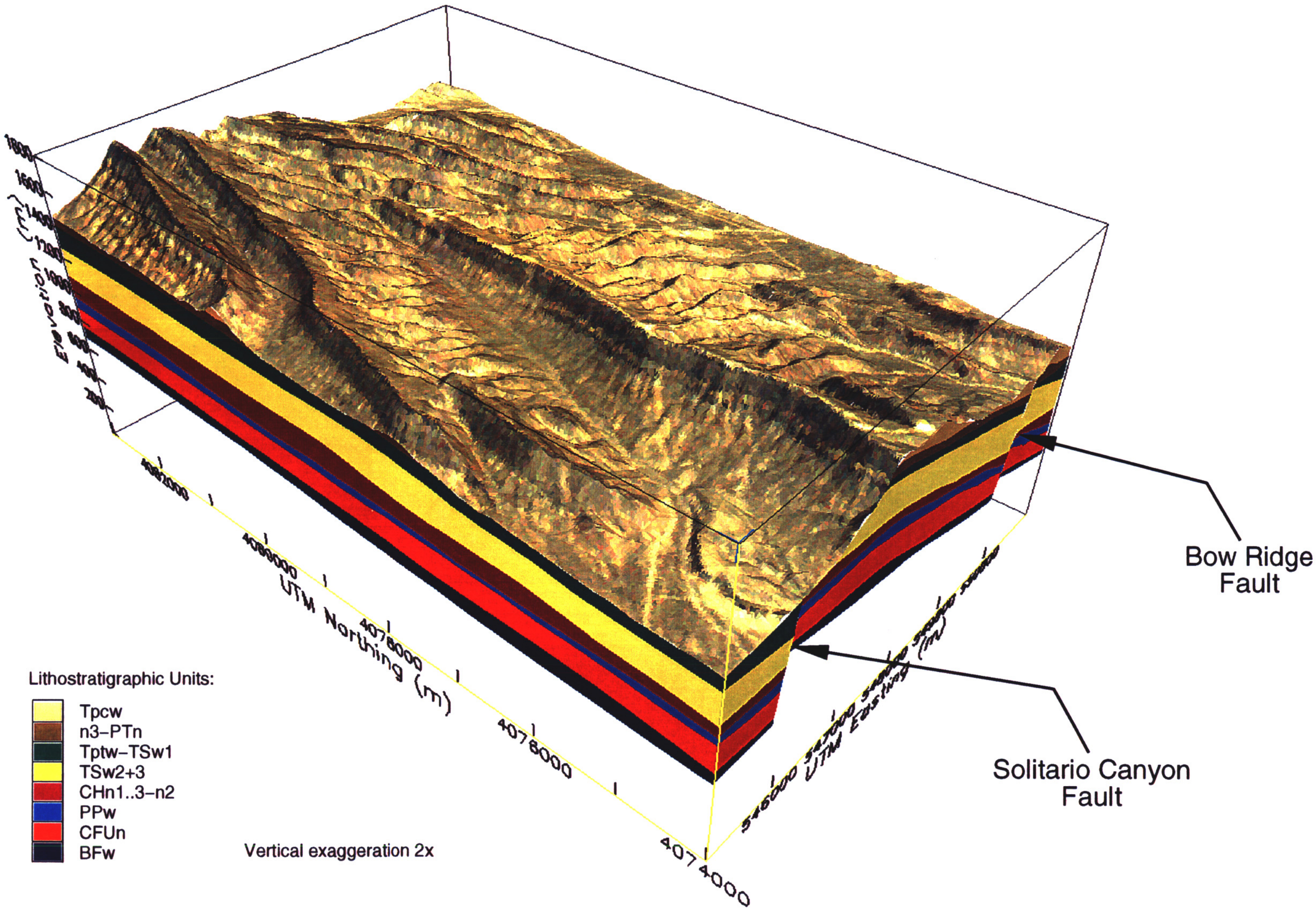

Figure 3–6. Landsat Thematic Mapper (TM) imagery superimposed over the surface of the 3D geological framework model

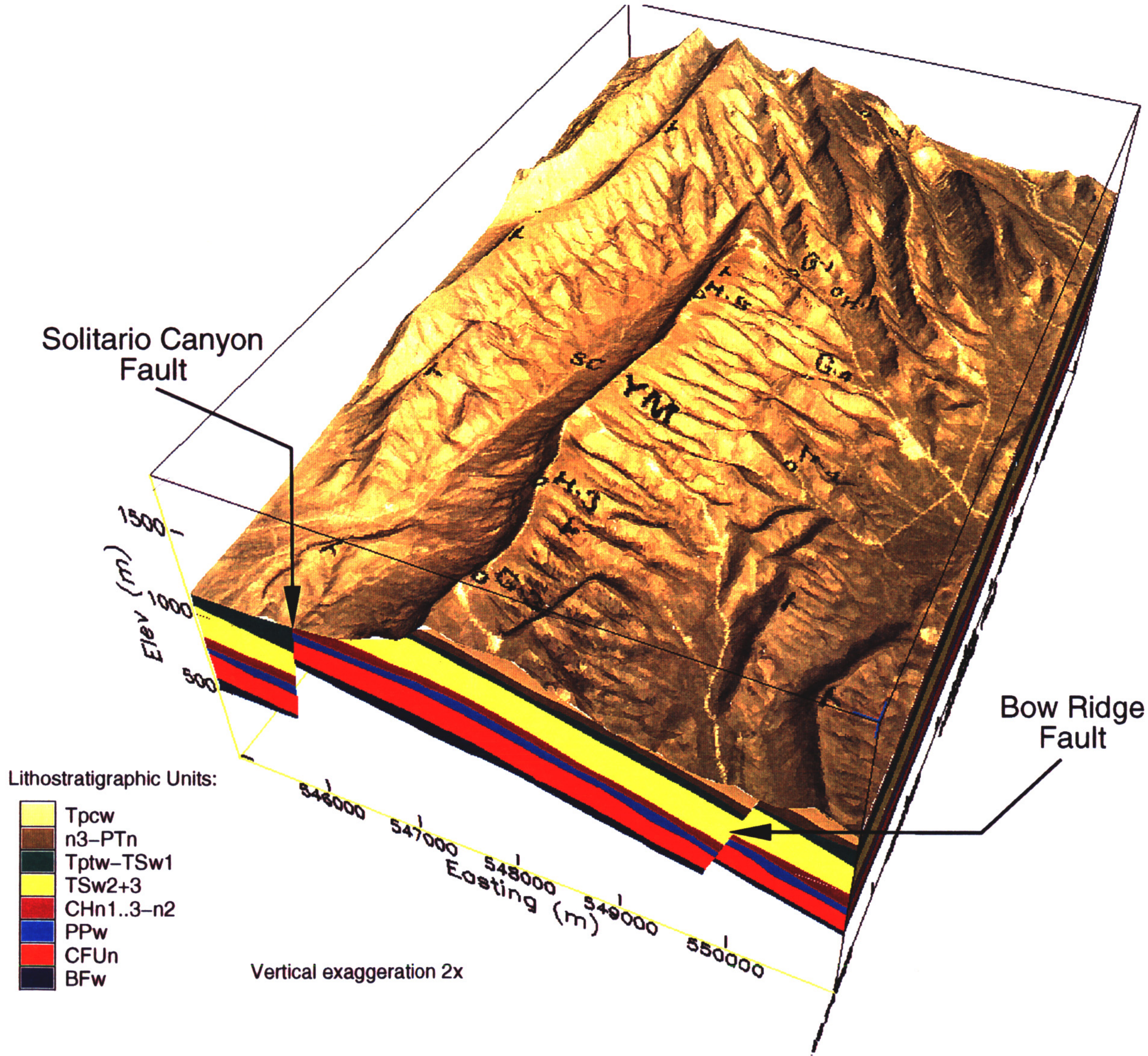

Figure 3–7. An aerial photographic image of Yucca Mountain superimposed over the surface of the 3D geological framework model

4 HYDROLOGIC APPLICATION FOR THE GEOLOGICAL FRAMEWORK MODEL—PRELIMINARY THREE-DIMENSIONAL HYDROSTRATIGRAPHIC MODELS

4.1 PURPOSE OF THE HYDROSTRATIGRAPHIC MODELS

The preliminary 3D hydrostratigraphic models, zoned lithologic layer-by-lithologic layer for porosity and saturated hydraulic conductivity, provide analysis tools for generating input data for use in groundwater flow models. The hydrostratigraphic models were constructed using field data collected during surface and subsurface investigations of the Yucca Mountain site by the DOE or its subcontractors and will be refined through incorporation of additional data as they become available. Hence, such models can be used by NRC staff during both prelicensing and licensing activities to assess the models chosen by the DOE for analysis of groundwater flow in relation to site suitability, design considerations, and potential repository performance. KTUs related to potentially adverse conditions associated with hydrologic considerations are defined in Section 3.2.2 (specifically, review plans 3.2.2.6, 3.2.2.8, 3.2.2.9, and 3.2.2.12) of the LARP (Nuclear Regulatory Commission, 1994). These KTUs make it important for NRC staff to be able to consider models provided by the DOE in light of how reasonably those models represent subsurface hydrologic conditions. The KTUs are at the level for which the LARP (Nuclear Regulatory Commission, 1994) requires detailed safety review supported by either analyses or independent tests and analyses. Therefore, it will be necessary for NRC staff to compare hydrologic models proposed by the DOE with an independently developed model to determine whether representation and explanation of subsurface hydrologic conditions are adequate and reasonable when documentation, logic, assumptions, bounding conditions, and bounding assessments for the DOE models are critically reviewed.

4.2 DESCRIPTION OF THE HYDROSTRATIGRAPHIC MODELS

Model construction approach, types and sources of data used in development and construction of the preliminary hydrostratigraphic models, and characteristics of the models are discussed in this section. Since the hydrologic parameters used to construct the hydrostratigraphic models (i.e., porosity and saturated hydraulic conductivity) were incorporated in the 3D geological framework model, boundaries of the models, topography, lithostratigraphy, fault zones, and the water table are represented in the same manner as described for the geological framework model (Section 3).

4.2.1 Model Construction Approach

Boreholes in which information on porosity and saturated hydraulic conductivity existed were few (i.e., twelve holes from which both parameters were taken and two additional holes from which only saturated hydraulic conductivity was taken). The greatest concentration of boreholes with these data (i.e., nine boreholes) was located in a cluster in the east-central part of the model (Figure 4-1). Sparseness of data and clustering of data points, coupled with the fact that the lithostratigraphic units exhibited internal variations in these two parameters that could not be directly equated to continuous subunits at this time (Appendix B), made it necessary to carefully consider how these two hydrologic parameters could best be represented in the 3D model. Three methodological approaches were tested for representing values of these parameters.

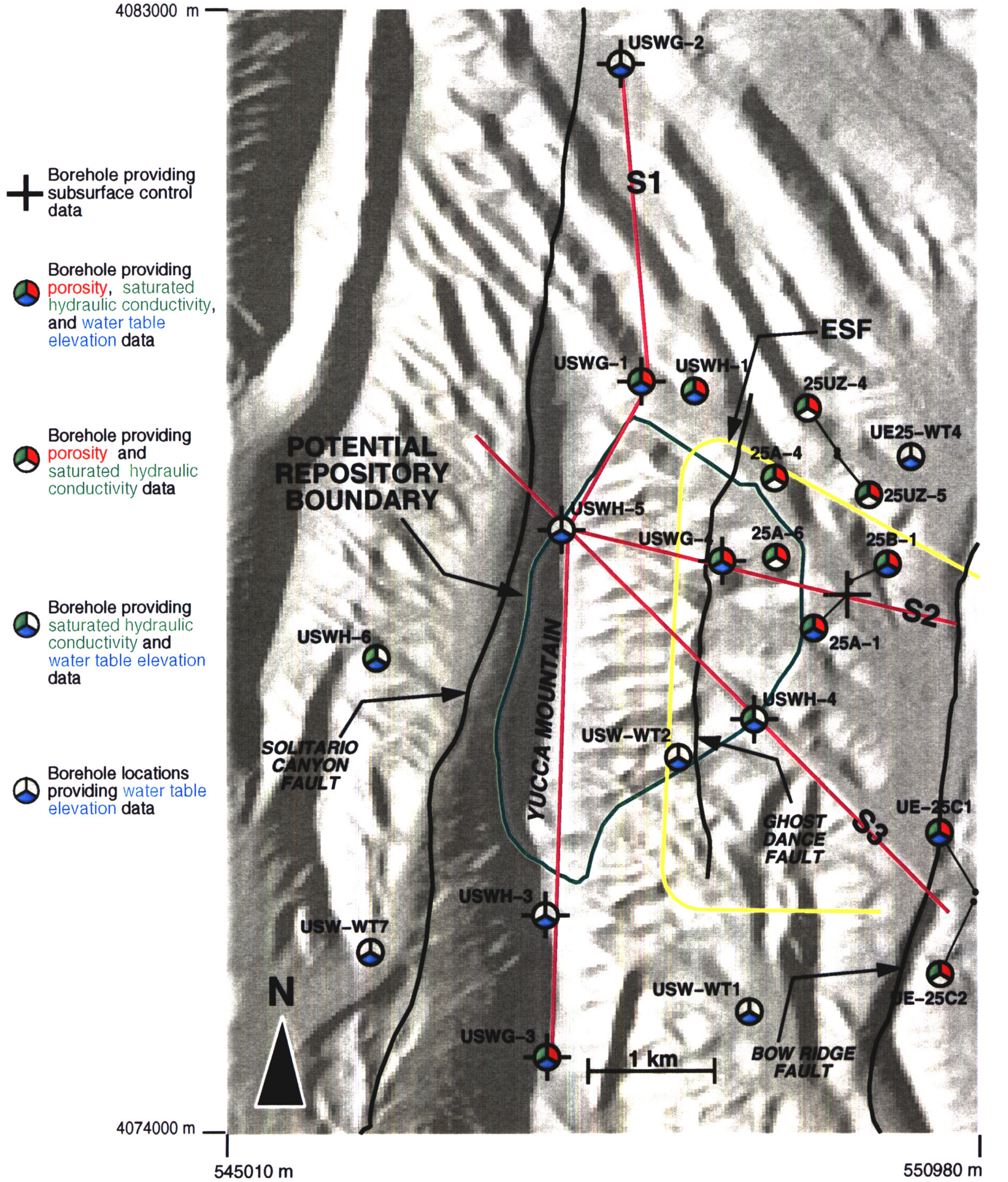

Figure 4–1. Locations of boreholes from which data on porosity and saturated hydraulic conductivity were taken within the boundaries of the CNWRA 3D geological framework model for Yucca Mountain. Locations of cross sections (S1, S2, S3) and boreholes providing subsurface control on lithostratigraphic units and faults and locations of boreholes from which water table elevation data were taken are also shown. Universal Transverse Mercator (UTM) coordinates are indicated.

The first method involved allowing EarthVision software to automatically interpolate property values between boreholes, using data on the same property from the nearest borehole, regardless of the lithologic unit in which the data were obtained (i.e., no unit control was exercised in the interpolation scheme). For the second approach, property values were automatically interpolated by EarthVision software using data from the nearest borehole, but within the same lithologic unit as that for the point being computed (i.e., unit control was exercised). The third method entailed defining input variables for the property values by computing the arithmetic mean (for porosity) or geometric mean (for saturated hydraulic conductivity) of the hydrologic parameters for each lithologic unit using borehole data from that specific unit. The values thus obtained for porosity and saturated hydraulic conductivity were held constant across the model for a given lithostratigraphic layer rather than permitting the algorithm in the EarthVision software to automatically extrapolate parameter values within the lithologic layers away from the known data points.

Test models were computed and compared for each approach. 3D models derived from the first two approaches exhibited distributions for the two hydrologic parameters that were highly anomalous because extrapolations were made with the software algorithm between less than fifteen boreholes that were clustered in the east-central part of the model. Therefore, the third method of modeling the values was selected to provide control on the values of porosity and saturated hydraulic conductivity assigned for the eight lithostratigraphic units comprising the 3D model. Using this approach then, the means are assumed to represent a reasonable "first cut" for modeling the hydrostratigraphic parameters in the model volume. Procedures for constructing the hydrostratigraphic models were the same as those for the 3D geological framework model (Section 3) except for the last stage of model construction wherein mean values for porosity and saturated hydraulic conductivity were entered for each lithologic unit using the EarthVision GSB tool (Dynamic Graphics, Inc., 1994b).

Regardless of the approach used for this preliminary hydrostratigraphic application, it is clearly recognized that data from additional boreholes distributed more evenly across the model volume would improve the parameter value representation. Additional borehole information on these two parameters may make it possible to illustrate variations in the parameters within layers as well as between layers, or to illustrate variations in these two parameters in, along, and across fault zones.

4.2.2 General Hydrostratigraphic Interpretations

Scott and Bonk (1984) interpreted the lithostratigraphic units shown in their original geological cross sections to reflect a relationship between degree of welding, fracturing, and hydraulic conductivity. Scott and Bonk (1984) formulated their interpretation based on information from Scott et al. (1983) which indicated welded units were highly fractured with high hydraulic conductivity, while non-welded units were less fractured and characterized by lower hydraulic conductivity. Scott and Bonk (1984) located lithostratigraphic contacts in the cross sections based on major changes in degree of welding of the volcanic tuff units rather than on petrologically-defined lithostratigraphic breaks. Consequently, non-welded units of Scott and Bonk (1984) may contain several petrographically distinct lithostratigraphic units. For example, non-welded materials occurring at the base of the Topopah Spring, in bedded tuffs, in the Calico Hills and Prow Pass, and at the top of the Bullfrog were considered to form one "unit" at some localities in their map area. Hence, the original Scott and Bonk (1984) cross sections, three of which were balanced and used in construction of the 3D geological framework model as described in Section 3.2.2, were considered to broadly illustrate differences in degree of welding between lithostratigraphic units. However, no quantitative data to illustrate ranges in hydraulic conductivity between welded (more fractured) and non-welded (less fractured) units were presented by Scott and Bonk (1984). Based on matrix saturated hydraulic conductivity data derived from borehole core samples, rather than bulk measurements derived from *in situ* testing, the hydrostratigraphic model for saturated hydraulic conductivity (Section 4.2.4) illustrates a different relationship between welded/non-welded units and saturated hydraulic conductivity than that proposed by Scott et al. (1983) and Scott and Bonk (1984). Generally, welded units in the hydrostratigraphic model have lower matrix hydraulic conductivities than do non-welded units. While inconsistencies in saturated hydraulic conductivity data can result if core samples tested do not adequately capture fractures or their effects on hydraulic conductivity, other investigators have also noted that welded units at Yucca Mountain have lower matrix hydraulic conductivity (and porosity) and non-welded units have higher matrix hydraulic conductivity and porosity (e.g., Montazer and Wilson, 1984; Wittwer, et al., 1992; Rautman and Robey, 1993).

Ortiz et al. (1985) presented a lithostratigraphy based on porosity and grain density that they broadly correlated with thermal, mechanical, and hydrological properties of the units. As was the case for Scott and Bonk (1984), however, no quantitative data were shown to illustrate relationships between the lithostratigraphic units and these properties. Also, degree of fracturing was not directly related to porosity by Ortiz et al. (1985), so relationships between fracturing, porosity, and degree of welding cannot be deduced from their data. Ortiz et al. (1985) considered non-welded (and zeolitized) units to possess high porosity and welded (and devitrified) units to be characterized by low porosity. Similar associations are clearly illustrated in the hydrostratigraphic model for porosity (Section 4.2.3).

No site-specific data exist at this time for defining hydrologic properties of fault zones at or near Yucca Mountain, so no variations in porosity or saturated hydraulic conductivity were incorporated at, along, or across the three faults included in the 3D hydrostratigraphic models. Acquisition and incorporation of hydrologic property data for the fault zones will be an important addition for later iterations of the hydrostratigraphic models. Other investigators have also pointed out the critical nature of field data for characterizing the hydrology of fault zones at Yucca Mountain in order to analyze groundwater flow and transport in the repository block (Wittwer et al., 1993; Tsang et al., 1993).

4.2.3 Data and Characteristics of the Porosity Model

Information drawn from USGS open-file and water resources investigations reports (Anderson, 1981, 1992; Rush et al., 1983; Lahoud et al., 1984; Flint and Flint, 1990) provide porosity data from twelve boreholes including UE25a#1, UE25a#4, UE25a#6, UE25b#1, UE25c#1, UE25c#2, UE25UZ#4, UE25UZ#5, USW G-1, USW G-4, USW GU-3/G-3, and USW H-1. Locations of boreholes from which hydrologic parameters (i.e., both porosity and saturated hydraulic conductivity) were taken are shown in Figure 4-1. Boreholes UE25a#1, USW G-1, USW G-4, USW GU-3 were four of the eight boreholes from which the 3D geological framework model was built (Section 3.2.3).

Appendix B presents detailed porosity and saturated hydraulic conductivity data from all boreholes, along with information on degree of welding as determined from borehole logs in the USGS report sources cited in the first paragraph of this section. Table 4-1 summarizes information from Appendix B by illustrating ranges in porosity values noted for the eight lithostratigraphic units, and the arithmetic means computed for each lithostratigraphic unit from those value ranges. Arithmetic means of measured ranges of porosity were computed to represent this parameter in the 3D hydrostratigraphic model because porosity values are distributed symmetrically with nearly equal arithmetic means and medians—a distribution that suggests the arithmetic mean is the appropriate measure of central tendency for this hydrologic variable.

Considering data shown in Appendix B and Table 4-1, a clear correlation exists between degree of welding and porosity as suggested by Ortiz et al. (1985) and other investigators (Montazer and Wilson, 1984; Wittwer, et al., 1992; Rautman and Robey, 1993). That is, welded units have lowest porosities. Also, detailed information included in Appendix B indicates some lithostratigraphic units (e.g., PPw and BFw) show both vertical (i.e., in a single borehole with depth) and lateral (i.e., between boreholes) variations in porosity that can probably be equated with differences in degree of welding. Even welded units have zones that are less welded, particularly near the top or base of a unit (e.g., Tpcw), as was reported by Scott and Bonk (1984). Additional borehole data may make it possible to delineate subunits of the eight lithostratigraphic units in the 3D model relative to porosity variations and associated degree of welding. No attempt was made to establish subunits at this time because of the sparseness of existing data.

The preliminary 3D hydrostratigraphic model illustrating unit-by-unit variations in porosity is shown in Figure 4-2. Table 4-2 summarizes the input data derived by taking the arithmetic mean of the ranges for porosity from Table 4-1. The repository unit (TSw2+3) clearly stands out in the lithostratigraphic sequence (Figure 4-2) because of the low porosity (i.e., 14 percent) of this welded unit. The unit with the highest porosity, greater than 40 percent, is non-welded unit n3-PTn (Figure 4-2). In general, correlation of porosity data with information on degree of welding indicates that moderately to densely welded units have porosities less than 25 percent and non-welded units have porosities greater than 30 percent (Appendix B). However, detailed information in Appendix B clearly illustrates that some lithostratigraphic units show both vertical and lateral variations in porosity that can probably be equated with differences in degree of welding. Whether there may be a contribution to porosity from fractures was not assessed, but core samples tested for porosity may not have captured such contributions, should they exist.

4.2.4 Data and Characteristics of the Saturated Hydraulic Conductivity Model

Saturated hydraulic conductivity data were derived from fourteen boreholes, including the same twelve used for porosity data (i.e., UE25a#1, UE25a#4, UE25a#6, UE25b#1, UE25c#1, UE25c#2, UE25UZ#4, UE25UZ#5, USW G-1, USW G-4, USW GU-3/G-3, and USW H-1), USW H-4 as described by Whitfield et al. (1985), and USW H-6 as described by Craig and Reed (1989). Locations of all boreholes from which hydrologic parameters (i.e., both saturated hydraulic conductivity and porosity) were taken are shown in Figure 4-1. USW H-4 was another of the eight boreholes used for subsurface control in the 3D geological framework model.

Appendix B presents detailed saturated hydraulic conductivity and porosity data from all boreholes, along with information on degree of welding as determined from borehole logs in the USGS report sources cited in the first paragraph of this section and in Section 4.2.3. Table 4-3 summarizes data from Appendix B by illustrating ranges in saturated hydraulic conductivity values noted for the eight lithostratigraphic units, and the geometric means computed for each lithostratigraphic unit from those value ranges. The geometric mean of measured ranges of saturated hydraulic conductivity was computed to represent this parameter in individual lithostratigraphic units of the 3D hydrostratigraphic model. This mean was chosen because it is considered to provide a representative value for permeability, a parameter to which hydraulic conductivity is related in hard rock materials (de Marsily, 1986).

Table 4-1. Data ranges and arithmetic means for matrix porosity as determined from USGS open-file and water resources investigations reports referenced in the text (Section 4.2.3). Data are keyed to the eight lithostratigraphic units included in the 3D geological framework model.

Lithostratigraphic Unit	Unit Designation in 3D Model	Number of Samples/Boreholes	Range	Median	Arithmetic Mean
Tiva Canyon	Tpcw	15/5	0.06–0.43	0.08	0.15
Yucca Mountain	n3-PTn	8/4	0.32–0.45	0.43	0.42
Pah Canyon	n3-PTn	5/3	0.41–0.48	0.46	0.45
Topopah Spring	Tptw-TSw1 & TSw2+3	76/6	—	—	—
undifferentiated	Tptw-TSw1 & TSw2+3	27	0.06–0.30	0.13	0.16
welded	Tptw-TSw1 & TSw2+3	48	0.03–0.28	0.14	0.14
non-welded	Tptw-TSw1 & TSw2+3	1	—	0.27	0.27
Calico Hills	CHn1..3-n2	24/8	0.14–0.47	0.31	0.30
Prow Pass	PPw	25/6	0.10–0.39	0.26	0.28
Crater Flat Upper	CFUn	6/2	0.23–0.33	0.29	0.29
Bullfrog	BFw	38/4	0.06–0.38	0.22	0.21

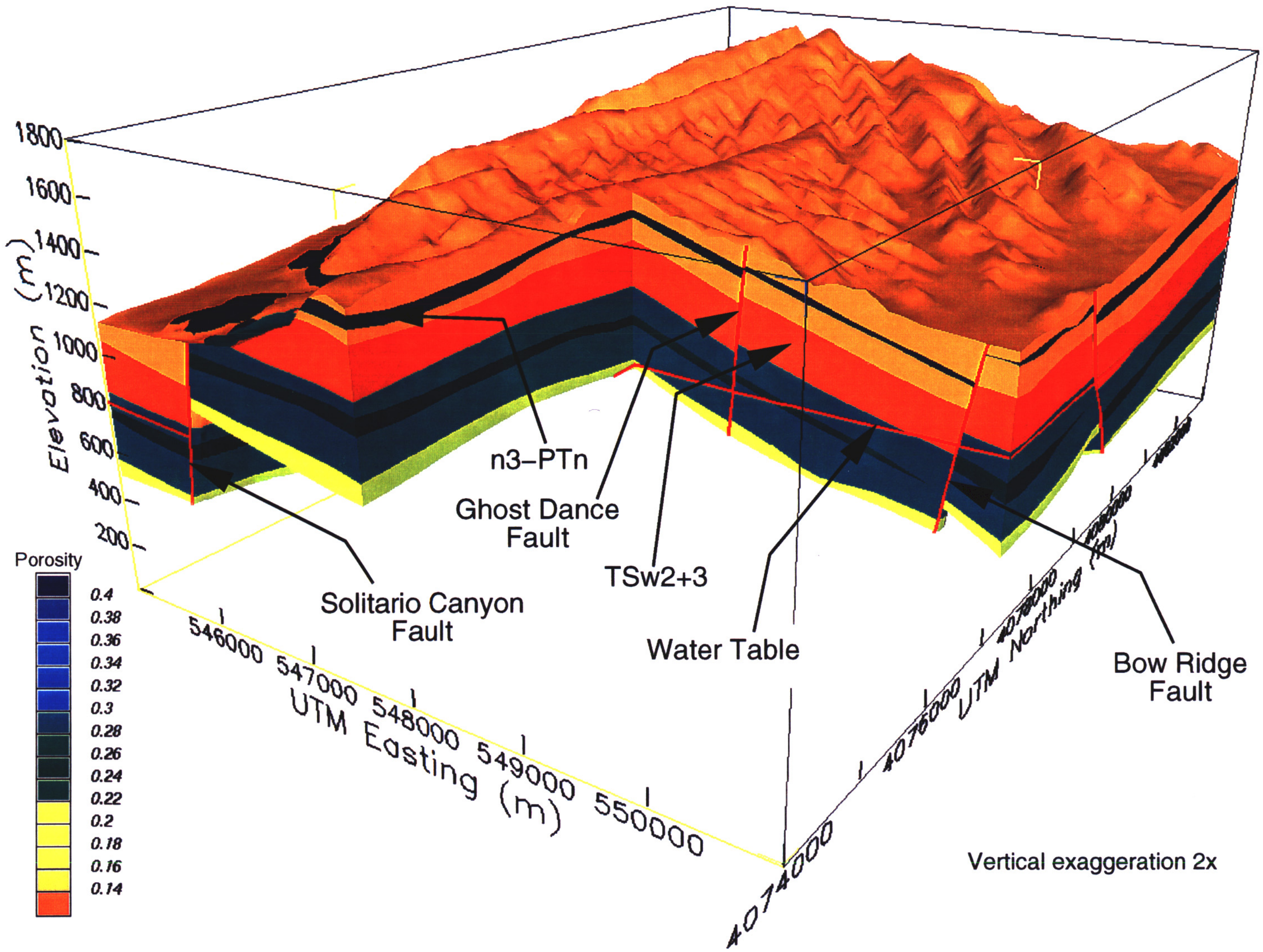

Figure 4–2. Perspective view of the CNWRA 3D porosity hydrostratigraphic model. Layering corresponds to the eight lithostratigraphic units comprising the 3D geological framework model.

Table 4-2. Summary of input data for the two hydrostratigraphic models presented in the report illustrating unit-by-unit variations in porosity (computed as arithmetic means) and saturated hydraulic conductivity (computed as geometric means)

Lithostratigraphic Unit	Unit Designation in 3D Model	Saturated Hydraulic Conductivity (matrix,m/s) [Geometric Mean]	Saturated Hydraulic Conductivity (bulk,m/s) [Geometric Mean]	Porosity (matrix) [Arithmetic Mean]
Tiva Canyon	Tpcw	1.5E-10	—	0.15
Yucca Mountain	n3-PTn	1.7E-07	—	0.42
Pah Canyon	n3-PTn	5.4E-08	—	0.45
Topopah Spring				
undifferentiated	Tptw-TSw1 & TSw2+3	2.4E-10	—	0.16
welded	Tptw-TSw1 & TSw2+3	8.5E-11	—	0.14
non-welded	Tptw-TSw1 & TSw2+3	6.8E-08*	—	0.27*
Calico Hills	CHn1..3-n2	4.8E-10	—	0.30
Prow Pass	PPw	1.4E-10	7.5E-06	0.26
Crater Flat Upper	CFUn	5.1E-10	—	0.29
Bullfrog	BFw	1.1E-09	3.4E-06	0.21

*single sample

Table 4-3. Data ranges and geometric means for saturated hydraulic conductivity as determined from USGS reports referenced in the text (Section 4.2.4). Data are keyed to the eight lithostratigraphic units included in the 3D geological framework model.

SATURATED HYDRAULIC CONDUCTIVITY, m/s (Matrix Values from Core Samples)					
Lithostratigraphic Unit	**Unit Designation in 3 D Model**	**Number of Samples/ Boreholes**	**Range (m/s)**	**Median**	**Geometric Mean**
Tiva Canyon	Tpcw	15/5	1.8E-12—1.4E-06	4.9E-11	1.5E-10
Yucca Mountain	n3-PTn	5/3	7.3E-09—2.3E-06	1.6E-07	1.7E-07
Pah Canyon	n3-PTn	4/2	6.6E-09—5.2E-07	1.0E-07	5.4E-08
Topopah Spring	Tptw-TSw1 & TSw2+3	50/5	—	—	—
undifferentiated	Tptw-TSw1 & TSw2+3	19	1.1E-11—1.6E-06	1.2E-10	2.4E-10
welded	Tptw-TSw1 & TSw2+3	30	9.7E-14—6.3E-08	9.0E-11	8.5E-11
non-welded	Tptw-TSw1 & TSw2+3	1	—	6.8E-08	6.8E-08
Calico Hills	CHn1..3-n2	18/7	4.4E-11—3.0E-07	2.6E-10	4.8E-10
Prow Pass	PPw	25/6	1.5E-11—4.6E-07	9E-10	1.4E-09
Crater Flat Upper	CFUn	6/2	3.8E-11—2.9E-09	5.5E-10	5.1E-10
Bullfrog	BFw	38/5	3.9E-12—1.1E-07	1.0E-09	1.1E-09
SATURATED HYDRAULIC CONDUCTIVITY, m/s (Bulk Values from *In-Situ* Tests)					
Prow Pass	PPw	4/2	3.8E-06—1.3E-05	8.4E-06	7.5E-06
Bullfrog	BFw	8/3	2.9E-08—4.8E-05	8.5E-06	3.4E-06

Considering data shown in Appendix B and Table 4-3, the correlation proposed by Scott et al. (1983) and Scott and Bonk (1984) of welded units exhibiting highest saturated hydraulic conductivities (i.e., because welded units were considered to be most fractured) is not apparent. Lack of this correlation may be an indication that values of matrix saturated hydraulic conductivity determined from core samples did not record the influence of fracturing on this parameter. Few *in situ* tests for bulk saturated hydraulic conductivity were run for the lithostratigraphic units included in the 3D model. Where *in situ* measurements were taken for units PPw and BFw, however, the following differences in geometric means were noted (Table 4-3): PPw (core) = 1.4E-09, PPw (*in situ*) = 7.5E-06; BFw (core) = 1.1E-09, BFw (*in situ*) = 3.4E-06. The higher *in situ* bulk values may reflect the presence and effects of fractures on saturated hydraulic conductivity in the welded parts of these two units as suggested by Scott et al. (1983) and Scott and Bonk (1984). Generally, however, variations in saturated hydraulic conductivity appear less systematic relative to degree of welding, particularly for core samples, and even opposite from the correlation suggested by Scott et al. (1983) and Scott and Bonk (1984). This opposite correlation of lower matrix saturated hydraulic conductivity associated with strong welding of units in the Yucca Mountain area has been recognized by other investigators (e.g., Montazer and Wilson, 1984; Wittwer, et al., 1992; Rautman and Robey, 1993)—a relationship also generally indicated by the data (Table 4-2) used to construct the preliminary 3D hydrostratigraphic model illustrating unit-by-unit variations in saturated hydraulic conductivity (Figure 4-3). The input data of Table 4-2 were derived by taking the geometric mean of the ranges for saturated hydraulic conductivity from Table 4-1. Because of the wide range of values exhibited by this parameter, the model (Figure 4-3) was constructed using log values. The repository horizon, welded unit TSw2+3, exhibits the lowest matrix saturated hydraulic conductivity (8.5E-11) and non-welded unit n3-PTn the highest (1.7E-07).

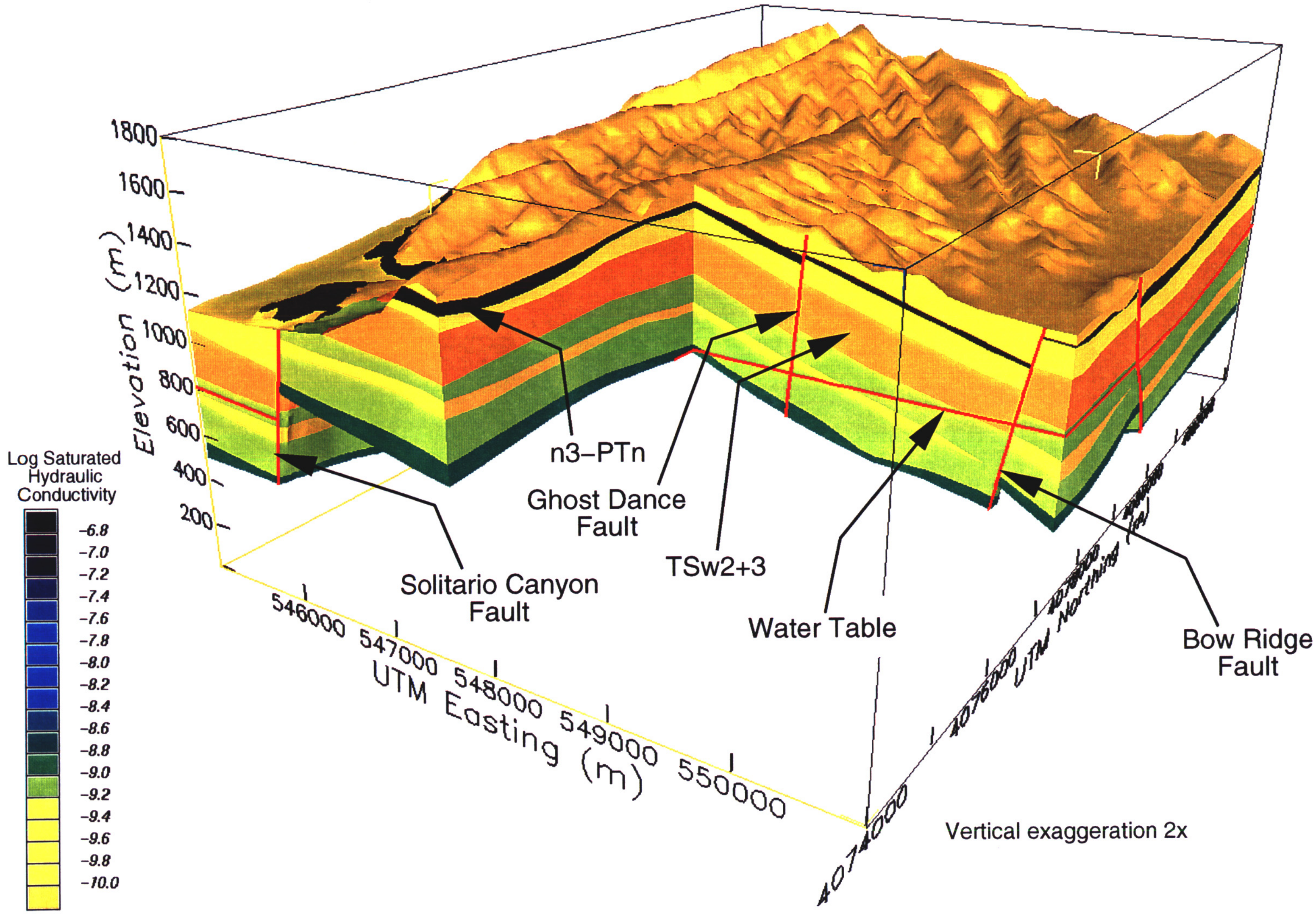

Figure 4–3. Perspective view of the CNWRA 3D saturated hydraulic conductivity hydrostratigraphic model. Layering corresponds to the eight lithostratigraphic units comprising the 3D geological framework model.

5 OTHER THREE-DIMENSIONAL MODELS OF THE YUCCA MOUNTAIN AREA

Several other 3D models of the Yucca Mountain area have been developed and used in either hydrologic or engineering applications. These models include a geostatistically based 3D model of lithostratigraphy developed by Sandia National Laboratory (SNL) for the second iteration of total system performance assessment (i.e., TSPA93) at Yucca Mountain (Wilson et al., 1994a); a conceptual 3D site-scale model of the unsaturated zone at Yucca Mountain being developed by Lawrence Berkeley Laboratory (LBL) in concert with the USGS (Wittwer et al., 1992); and a 3D lithostratigraphic model for Yucca Mountain being developed by the USGS using software from LYNX Geosystems, Incorporated (Buesch, et al., 1993). These three specific models are discussed in this section.

5.1 THE SANDIA NATIONAL LABORATORY GEOSTATISTICALLY BASED STRATIGRAPHIC MODEL

In the geostatistically based 3D stratigraphic model developed by SNL for TSPA93 (Wilson et al., 1994a), methods presented by Journel and Huijbregts (1978) and Clarke (1979) were used to incorporate site-specific borehole information on the welded and non-welded stratigraphic units comprising the model. In the repository region, 22 boreholes, as listed in Schenker et al. (1994), were used to provide subsurface data on thicknesses and distribution of both welded and non-welded units. These data were characterized by an uneven spatial distribution because fewer boreholes occurred in the western part of the model area and boreholes in the eastern part were strongly clustered. Also, the unbalanced geological cross sections of Scott and Bonk (1984) were digitized to provide information on subsurface distribution of welded and non-welded stratigraphic units for generating the spatial continuity model of the units and for representing offset of the units by the Ghost Dance fault, the only structure included in the model. Using geostatistical techniques and these data, boundaries between welded and non-welded units were consequently defined, spatial distributions of unit thicknesses were determined, and representations of subsurface stratigraphy of the potential repository area were developed. Wilson et al. (1994a) concluded that boreholes from which data were drawn were not spaced closely enough for accurate predictions of strata contacts and thicknesses, since significant variations were noted in positions of strata contacts for the geostatistical model simulations undertaken during development of the 3D model.

Lithostratigraphic units were equated with hydrologic properties based on degree of welding as was done by Scott and Bonk (1984) and Ortiz et al. (1985). For example, more densely welded materials were characterized by lower matrix porosities than were the non-welded to poorly welded units. Although unit thicknesses varied, hydrologic parameters were assumed to be independent of unit thickness so that parameters were considered applicable throughout a specific hydrostratigraphic unit. The lithostratigraphic/hydrostratigraphic units in the model included a non-welded Bullfrog and welded Tram below the welded Bullfrog (BFw in the CNWRA model) for a total of ten units rather than eight as represented in the CNWRA model. East-west boundaries of the TSPA93 model were somewhat narrower than for the CNWRA 3D model and extended from Solitario Canyon on the west to just beyond the perimeter drift on the east. For direct comparison of model boundaries with those of the CNWRA model (Table 3-1), locations of the corners of the TSPA93 model boundaries were defined by the following NSP coordinates, given in feet: 555,205 and 565,155 east; 757,620 and 769,520 north.

For application of the geostatistically based 3D stratigraphic model to hydrology, probabilistic calculations for describing flow through an equivalent porous medium in a composite-porosity model (represented as a 2D stratigraphic profile developed from the 3D model) were conducted using a simplified reference stratigraphy (Wilson et al., 1994b). This reference stratigraphy was selected from results of the ten, fully 3D, geostatistical simulations that were undertaken to define lithostratigraphy and hydrostratigraphy in the subsurface. Hydrologic properties were picked from probability distribution functions (PDFs). Consequently, the models exercised for probabilistic analyses were abstracted from results of the data development and geostatistical stratigraphic modeling activities. Specifically, for representation of stratigraphy, eight stratigraphic profiles were extracted from the fully 3D, geostatistically based, stochastic models and simplified, and then one of these stratigraphic profiles was used to represent stratigraphy in the TSPA93 calculations for analyzing 2D unsaturated-zone groundwater flow and transport in the composite-porosity model. For hydrologic data, more than a dozen hydrologic parameters from three categories (i.e, matrix, bulk, and fracture—and specifically including porosity and saturated hydraulic conductivity) were treated in TSPA93. Each hydrologic property was considered homogeneous so that a single PDF was developed for each property in each of the ten hydrostratigraphic units. The application in TSPA93 concerned with 3D modeling of the saturated zone, also discussed by Wilson et al. (1994a), was undertaken in a model not directly related to the geostatistically based stratigraphic model of the unsaturated zone.

5.2 THE LAWRENCE BERKELEY LABORATORY/U.S. GEOLOGICAL SURVEY SITE-SCALE MODEL

In the LBL/USGS conceptual 3D site-scale model described by Wittwer et al. (1992), the unsaturated zone at Yucca Mountain was modeled in terms of hydrostratigraphy, structure, moisture infiltration, and rock properties. The model covered an area of about 30 sq km centered around the potential repository. It was bounded by the Bow Ridge fault to the east and the Solitario Canyon fault to west, and extended north to Yucca Wash. Structures represented were taken from Scott and Bonk (1984) and Nimick and Williams (1984) and included the Ghost Dance, Abandoned Wash, and Dune Wash faults. The faults were accounted for by simulation of vertical offsets in the model using displacement amounts determined from information in Scott and Bonk (1984) and Nimick and Williams (1984).

Hydrostratigraphic unit boundary elevations taken from 23 boreholes were combined with data on dips and strikes of lithologic units from Scott and Bonk (1984) and Nimick and Williams (1984) to provide consistency between surface and subsurface data. The bottom of the model coincided with the water table because only the unsaturated zone was modeled. The four major hydrostratigraphic units modeled in the unsaturated zone included: (i) welded Tiva Canyon; (ii) non-welded Paintbrush; (iii) welded Topopah Spring; and, (iv) non-welded Calico Hills.

Wittwer et al. (1992) regarded welded tuffs (e.g., like the Tiva Canyon and Topopah Spring units) to be characterized by low porosities (10 to 15 percent) and low saturated matrix hydraulic conductivities ($2–4 \times 10^{-11}$ m/s). They characterized welded tuffs to have high fracture densities (8–40 fractures/m^3). Conversely, Wittwer et al. (1992) considered non-welded and bedded tuffs (e.g., the nonwelded Paintbrush) to have higher matrix porosities of 25 to 50 percent; higher saturated hydraulic conductivities of 10^{-6} to 6^{-8}–10^{-8} m/s; and lower fracture densities of about 1 fracture/m^3. They developed these values for porosity, saturated hydraulic conductivity, and fracture density based on information derived from Montazer and Wilson (1984), Flint and Flint (1990), and Scott et al. (1983).

Wittwer et al. (1992) considered the most critical issue in development of the site-scale model of Yucca Mountain to be the poorly known flow characteristics of the major faults and recognized the importance of sufficient field data for prescribing fault hydrologic properties. A follow-up effort by Wittwer et al. (1993) analyzed the role of fault zones on fluid flow using the unsaturated zone model of Wittwer et al. (1992) for running 2D simulations using TOUGH2 (Pruess, 1990) software. The purpose of the modeling by Wittwer et al. (1993) was to derive results of steady-state simulations performed with a 2D numerical grid that represented the hydrogeology of the site. They modeled seventeen non-uniform layers representing the lithologic variations in the four main welded and nonwelded hydrostratigraphic units (i.e., welded Tiva Canyon, non-welded Paintbrush, welded Topopah Spring, and non-welded Calico Hills). The three fault zones (i.e., the Ghost Dance, Abandoned Wash, and Dune Wash faults) were explicitly modeled as porous media with either very high or very low permeability relative to neighboring lithologic units. Such bounding calculations were used because of the lack of data on fault hydrologic properties. Cross sections extracted from the 3D site-scale model of Wittwer et al. (1992) were used to illustrate the geometry and distributions of hydrostratigraphic units and their sublayers in 2D, along with variability in rock properties. Results were interpreted in terms of the influence of major fault zones on potential occurrence and intensity of vertical and lateral moisture flow and the existence of preferential flow pathways. For a permeable fault, the characteristics curves assumed by Wittwer et al. (1993) resulted in relatively low capillary pressures and very low liquid saturations at steady-state such that flow from adjacent formations did not enter the fault and some of the infiltration prescribed at the top of the fault was lost into the surrounding lithologic units. Wittwer et al. (1993) pointed out that significant vertical flow in a fault would occur only if the characteristics curves for the fault were similar to those for adjacent formations and the absolute saturated permeability of the fault was significantly larger.

Tsang et al. (1993) also stressed the need for field measurements on hydrologic characteristics of fault zones in order to be able to determine the significance of faults in controlling flow and transport at Yucca Mountain, since the magnitude of flow in a fault zone depends on hydrologic properties of the zone. They modeled the Ghost Dance fault zone in a 2D east-west vertical section model and concluded that, if the fault zone were treated as a high-permeability, single- or double-porosity medium and if the capillary suction of the zone had the same dependence between saturated permeability and a capillary scaling parameter as the adjacent rocks, then the fault zone would have little effect on channeling or enhancing downward flow. However, they pointed out that, if the hydrologic properties of the fault zone were such that a larger saturated permeability were coupled to a stronger capillary action, then the zone could play a more important role in enhancing channeled flow. Consequently, Tsang et al. (1993) concluded that use of actual field data was very important for analyzing hydrologic flow in faults.

5.3 THE U.S. GEOLOGICAL SURVEY LYNX GEOSYSTEMS LITHOSTRATIGRAPHIC MODEL

In the preliminary USGS 3D lithostratigraphic model for Yucca Mountain constructed using LYNX Geosystems software (Buesch et al., 1993), the model was bounded on the west by the Solitario Canyon fault, on the east by the Bow Ridge fault, on the north by Yucca Wash, and on the south by an east-west line drawn through borehole USWG-3. As such, model area was consistent with that of the model constructed by Wittwer et al. (1992) and generally consistent (although somewhat more constricted west of the Solitario Canyon fault) with the model boundaries of the CNWRA 3D geological framework model.

Initial modeling efforts were focused on the Topopah Spring unit because it is the principal host rock of the potential repository. Seven subunits of the Topopah Spring were modeled and approximately 30 drillholes were used for subsurface control in the model. Fault zones other than the Solitario Canyon and Bow Ridge included the Ghost Dance/Abandoned Wash and Sever Wash faults, plus other un-named faults derived from Scott and Bonk (1984). Results from more recent mapping efforts (Spengler et al., 1993) were also used to define complexity of faults represented. A total of 25 faults (representing both northeast and northwest-trending structures) with displacements greater than 20 ft were included, compared to only six faults in the unsaturated zone model of Wittwer et al. (1992 and 1993) and three faults in the current CNWRA model. Buesch et al. (1993) considered their model to set the stage for more thorough investigations of the role of faulting in the future. The 3D model constructed by Buesch et al. (1993) has already been exercised to generate cross sections that were provided to ESF design engineers.

6 POTENTIAL REFINEMENTS AND APPLICATIONS FOR THE THREE-DIMENSIONAL GEOLOGICAL FRAMEWORK MODEL

In this section, concepts related to both continued refinement and modification of the 3D geological framework model and possible applications of the model other than those presented in Section 4 of this report are outlined. Updated versions of the 3D model with associated databases and documentation files will be developed and provided to the NRC on a mutually agreeable schedule as additional data are made available to the NRC by the DOE. Additional applications of the model will be accomplished as required with results also provided to the NRC.

6.1 MODEL REFINEMENTS

The 3D geological framework model discussed in this report will be refined and modified as additional pertinent data are collected and provided to the NRC by the DOE, gleaned from the existing DOE database, and obtained from published literature. The following specific refinements are being considered for incorporation into the next version of the model:

- Extend boundaries of the model at least far enough to encompass the 5-km compliance boundary around the potential repository. This refinement will make the model more practical for use in NRC/CNWRA Iterative Performance Assessment (IPA) studies.

- Construct a minimum of two new geological cross sections and to provide additional subsurface control on tops of lithostratigraphic units and positions of fault surfaces.

- Add more faults as appropriate, including northwest-trending and additional northeast-trending structures. Inclusion of additional faults may prove useful for analysis of Key Technical Issues (KTIs) related to structural deformation and seismicity and hydrologic characterization of structural features.

- Add alluvium to show its distribution and thickness. Inclusion of alluvium may prove important for infiltration studies in the CNWRA subregional hydrology research project.

- Refine depths to lithostratigraphic horizons and fault surfaces using data from additional boreholes and the two new cross sections to establish more control points on elevations of the tops of lithostratigraphic units and positions of fault surfaces. Modification of the 3D geological framework model is probable when data from additional boreholes can be used to provide finer constraints on depths and thicknesses of lithostratigraphic units and positions of fault surfaces where only digitized, structural contour data now exist.

Priorities assigned to these potential refinements will be established in accordance with the needs of the NRC.

6.2 MODEL APPLICATIONS

Applications of the 3D geological framework model include incorporating and displaying various types of data (e.g., engineering, geochemical, and hydrologic properties) for visually analyzing spatial distributions of properties in the 3D model; displaying and analyzing data pertinent to KTIs that the NRC deems necessary for the DOE to resolve; and extracting data from the 3D model for export and use in rigorous 2D analyses.

For an engineering application, the ESF tunnel can be added to the model to display subsurface intersections of the tunnel with lithostratigraphic units and faults. Also, rock mechanics and geochemical properties of lithologic units from borehole data and laboratory tests can be incorporated and displayed to analyze variations in the properties either within zones of the modeled volume or in the entire modeled volume.

Considering hydrologic applications, hydrologic data from *in situ* borehole tests (bulk properties) and laboratory tests on core samples (matrix properties) can be incorporated to display and visually analyze unit-by-unit variations in the hydrologic properties in a fashion similar to that accomplished for porosity and saturated hydraulic conductivity in Section 4. Hydrologic information for the Ghost Dance and other faults can be included in the model for displaying and visually analyzing variations along, across, and in fault zones if appropriate data are collected by the DOE and made available to the NRC. Even without specific hydrologic data from the fault zones, end-member models could be constructed using data from faults collected at other locations that treated the structures as high- and low-permeability zones for test case runs analyzing groundwater movement in 2D cross sections extracted from the 3D model similar to the analyses conducted by Wittwer et al. (1993). In addition, the ability to construct and display Allan diagrams (Allan, 1989) using the EarthVision 3D viewer tool makes it possible to visually analyze the intersections of fault surfaces with lithostratigraphic and hydrostratigraphic units and consider potential 3D hydrologic flow pathways which may be related to the faults. Alternative tectonic models also can be analyzed in relation to how structures are represented in the 3D model.

There are several KTIs that the NRC deems necessary for the DOE to resolve in order to prepare an acceptable license application which it may be possible to address using the 3D geological framework model. One may focus on issues related to structural deformation and seismicity, hydrologic characterization of structural features, and the ESF by incorporating appropriate data into the 3D model for close examination and visual analysis. These data can be extracted from the 3D model files, exported as 3D volume files and 2D cross sections, and used as input files, for example, for 2D geostatistical and flow model applications. Because the 3D model serves as a framework in which various types of data can be exhibited to determine distributions of properties relative to the lithostratigraphic units, it may also prove useful for facilitating integration of component fields when assessing KTIs.

7 REFERENCES

Allan, U.S. 1989. Model for Hydrocarbon Migration and Entrapment within Faulted Structures. *The American Association of Petroleum Geologists Bulletin* 73(7): 803–811.

Anderson, L.A. 1981. *Rock Property Analysis of Core Samples from the Yucca Mountain UE25a1 Borehole, Nevada Test Site, Nevada*. U.S. Geological Survey Open-File Report 81-1338. Denver, CO: U.S. Geological Survey.

Anderson, L.A. 1992. *Water Permeability and Related Rock Properties Measured on Core Samples from the Yucca Mountain USW GU-2/G-3 and G-4 Boreholes, Nevada Test Site, Nevada*. U.S. Geological Survey Open-File Report 92-201. Denver, CO: U.S. Geological Survey.

Buesch, D.C., R.P. Dickerson, R.M. Drake, and R.W. Spengler. 1994. Integrated geology and preliminary cross sections along the north ramp of the Exploratory Studies Facility, Yucca Mountain. *Proceedings of the Fifth Annual International Conference on High Level Radioactive Waste Management*. La Grange Park, IL: American Nuclear Society: 1,055–1,065.

Buesch, D.C., R.W. Spengler, J.E. Nelson, and R.P. Dickerson. 1993. Three-dimensional lithostratigraphic model at Yucca Mountain, Nevada: A framework for fluid transport modeling and engineering design. *Proceedings of the Topical Meeting on Site Characterization and Model Validation, FOCUS '93*. La Grange Park, IL: American Nuclear Society: 226–231.

Clark, L. 1979. *Practical Geostatistics*. New York, NY: Elsevier Applied Scientific Publishers.

CogniSeis Development, Inc. 1991. *GEOSEC (Version 2.0) User's Manual*. Houston, TX: CogniSeis Development, Inc.

Craig, R.W. and R.L. Reed. 1989. *Geohydrology of Rocks Penetrated by Test Well USW H-6, Yucca Mountain, Nye County, Nevada*. U.S. Geological Survey Water Resources Investigations Report 89-4025. Denver, CO: U.S. Geological Survey.

Dahlstrom, C.D.A. 1969. Balanced cross sections. *Canadian Journal of Earth Science* 6: 743–757.

de Marsily, G. 1986. *Quantitative Hydrology—Groundwater Hydrology for Engineers*. Orlando, FL: Academic Press, Inc., Harcourt-Brace-Jovanovich, Publishers.

Dickerson, R.P. and R.W. Spengler. 1994. Structural character of the northern segment of the Paintbrush Canyon fault, Yucca Mountain, Nevada. *Proceedings of the Fifth Annual International Conference on High Level Radioactive Waste Management*. La Grange Park, IL: American Nuclear Society: 2,367–2,372.

Dynamic Graphics, Inc. 1994a. *EarthVision (Version 2.0) User's Guide*. Alameda, CA: Dynamic Graphics, Inc.

Dynamic Graphics, Inc. 1994b. *EarthVision (Version 2.9 beta) User's Guide*. Alameda, CA: Dynamic Graphics, Inc.

Flint, L.E., and A.L. Flint. 1990. *Preliminary Permeability and Water-Retention Data for Nonwelded and Bedded Tuff Samples, Yucca Mountain, Nye County, Nevada*. U.S. Geological Survey Open-File Report 90-569. Denver, CO: U.S. Geological Survey.

Fridrich, C.J., W.W. Dudley, Jr., and J.S. Stuckless. 1994. Hydrogeologic analysis of the saturated-zone ground-water system under Yucca Mountain, Nevada. *Journal of Hydrology* 154: 133–168.

Journel, A.G., and Ch.J. Huijbregts. 1978. *Mining Geostatistics*. New York, NY: Academic Press.

Lahoud, R.G., D.H. Lobmeyer, and M.S. Whitfield. 1984. *Geohydrology of Volcanic Tuff Penetrated by Test Well UE-25b#1, Yucca Mountain, Nevada*. U.S. Geological Survey Water Resources Investigations Report 84-4253. Denver, CO: U.S. Geological Survey.

Montazer, P., and W.E. Wilson. 1984. *Conceptual Hydrologic Model of Flow in the Unsaturated Zone, Yucca Mountain, Nevada*. Water Resources Investigations Report 84-4355. Denver, CO: U.S. Geological Survey.

Nimick, F.B., and R.L. Williams. 1984. *A Three-Dimensional Geologic Model of Yucca Mountain, Southern Nevada*. SAND83-2593. Albuquerque, NM: Sandia National Laboratories.

Nuclear Regulatory Commission. 1994. *License Application Review Plan (LARP) for a Geologic Repository for Spent Nuclear Fuel and High Level Radioactive Waste*. NUREG-1323, Rev 0. Washington, D.C.: Nuclear Regulatory Commission: Division of Waste Management, Office of Nuclear Material Safety and Safeguards.

Ortiz, T.S., R.L. Williams, F.B. Nimick, B.C. Whittet, and D.L. South. 1985. *A Three-Dimensional Model of Reference Thermal/Mechanical and Hydrological Stratigraphy at Yucca Mountain, Southern Nevada*. SAND84-1076. Albuquerque, NM: Sandia National Laboratories.

Pruess, K. 1990. *TOUGH2-A General-Purpose Numerical Simulator for Multiphase Fluid and Heat Flow*. LBL-29400. Berkeley, CA: Lawrence Berkeley Laboratory.

Rautman, C.A. and T.H. Robey. 1993. Recent developments in stochastic modeling and upscaling of hydrologic properties in tuff. *Proceedings of the Fourth Annual International Conference on High Level Radioactive Waste Management*. La Grange Park, IL: American Nuclear Society: 1437–1445.

Robison, J.H. 1984. *Ground-Water Level Data and Preliminary Potentiometric Surface Maps, Yucca Mountain and Vicinity, Nye County, Nevada*. Water Resources Investigations Report 84-4197. Denver, CO: U.S. Geological Survey.

Rush, F.E., W. Thordarson, and L. Bruckheimer. 1983. *Geohydrologic and Drill-Hole Data for Test Well USW H-1, Adjacent to Nevada Test Site, Nye County, Nevada*. U.S. Geological Survey Open-File Report 83-141. Denver, CO: U.S. Geological Survey.

Schenker, A.R., D.C. Guerin, and T.H. Robey. 1994. *Stratigraphy and Hydrogeologic Properties Development for the Total-System Performance Assessment 1993*. SAND94-0244. Alburqerque, NM: Sandia National Laboratories.

Scott, R.B. and J. Bonk. 1984. *Preliminary Geologic Map (1:12,000 scale) of Yucca Mountain, Nye County, Nevada, with Geologic Cross Sections*. U.S. Geological Survey Open-File Report 84-494. Denver, CO: U.S. Geological Survey.

Scott, R.B., R.W. Spengler, S. Diehl, A.R. Lappin, and M.P. Chornack. 1983. Geologic character of tuffs in the unsaturated zone at Yucca Mountain, southern Nevada. Role of the Unsaturated Zone in Radioactive and Hazardous Waste Disposal. J.W. Mercer, P.S.C. Rao, and I.W. Marine, eds. *Science*: 289–335.

Spengler, R.W., C.A. Braun, R.M. Linden, L.G. Martin, D.M. Ross-Brown, and R.L. Blackburn. 1993. Structural characteristics of the Ghost Dance fault, Yucca Mountain, Nevada. *Proceedings of the Fourth Annual International Conference on High Level Radioactive Waste Management*. La Grange Park, IL: American Nuclear Society: 653–659.

Spengler, R.W., C.A. Braun, L.G. Martin, and C.W. Weisenberg. 1994. *The Sundance fault—A newly-recognized shear zone at Yucca Mountain, Nevada*. US Geological Survey Open-File Report 94-49. Denver, CO: U.S. Geological Survey.

Stirewalt, G.L. and D.B. Henderson. 1995. A preliminary three-dimensional geological framework model for Yucca Mountain. *Proceedings of the Sixth Annual International High Level Radioactive Waste Management Conference*. La Grange Park, IL: American Nuclear Society: 116–118.

Stirewalt, G.L., S.R. Young, and D.B. Henderson. 1994. *A Preliminary Three-Dimensional Geological Framework Model for Yucca Mountain, Nevada—Report to Accompany Model Transfer to the Nuclear Regulatory Commission*. CNWRA Report 94-023. San Antonio, TX: Center for Nuclear Waste Regulatory Analyses.

Tsang, Y.W., K. Pruess, and J.S.Y. Wang. 1993. *The Role of Fault Zones in Affecting Multiphase Flow at Yucca Mountain*. Berkeley, CA: Lawrence Berkeley Laboratory.

Whitfield, M.S., E.P. Eshom, W. Thordarson, and D.H. Schaefer. 1985. *Geohydrology of Rocks Penetrated by Test Well USW H-4, Yucca Mountain, Nye County, Nevada*. U.S. Geological Survey Water Resources Investigations Report 85-4030. Denver, CO: U.S. Geological Survey.

Wilson, J.L., J.H. Gauthier, R.W. Barnard, G.E. Barr, H.A. Dockery, et al. 1994a. *Total-System Performance Assessment for Yucca Mountain—SNL Second Iteration (TSPA-1993), Volume 1*. SAND93-2675. Albuquerque, NM: Sandia National Laboratories.

Wilson, J.L., J.H. Gauthier, R.W. Barnard, G.E. Barr, H.A. Dockery, et al. 1994b. *Total-System Performance Assessment for Yucca Mountain—SNL Second Iteration (TSPA-1993), Volume 2*. SAND93-2675. Albuquerque, NM: Sandia National Laboratories.

Wittwer, C.S., G.S. Bodvarsson, M.P. Chornack, et al. 1992. Design of a three-dimensional site-scale model for the unsaturated zone at Yucca Mountain, Nevada. *Proceedings of the Third International Conference on High Level Radioactive Waste Management*. La Grange Park, IL: American Nuclear Society 1: 263–271.

Wittwer, C.S., G. Chen, and G.S. Bodvarsson. 1993. Studies of the role of fault zones on fluid flow using the site-scale numerical model of Yucca Mountain. *Proceedings of the Fourth International Conference on High Level Radioactive Waste Management*. La Grange Park, IL: American Nuclear Society 1: 667–674.

Woodward, N.B., S.E. Boyer, and J. Suppe. 1989. *Balanced geological cross sections—An essential technique in geological research and exploration*. American Geophysical Union Short Course in Geology 6. Washington, D.C.: American Geophysical Union.

Young, S.R., G.L. Stirewalt, and R.A. Ratliff. 1991. Computer-assisted geometric and kinematic analysis of subsurface faulting in the vicinity of Yucca Mountain, Nevada, using balanced geologic cross sections. *Proceedings of the Second Annual International High Level Radioactive Waste Management Conference*. La Grange Park, IL: American Nuclear Society: 248–259.

Young, S.R., G.L. Stirewalt, and A.P. Morris. 1992. *Geometric models of faulting at Yucca Mountain*. CNWRA Report 92-008. San Antonio, TX: Center for Nuclear Waste Regulatory Analyses.

APPENDIX A

EARTHVISION FILES BEING TRANSFERRED TO THE NUCLEAR REGULATORY COMMISSION WITH THIS REPORT ON THE THREE-DIMENSIONAL GEOLOGICAL FRAMEWORK MODEL AND PRELIMINARY HYDROSTRATIGRAPHIC MODELS

Filename	Size(bytes)	Checksum	Blocks	Lines
Data Files				
boreholes.pdat	150977	21446	295	1416
flt010_bowRidge010_jan23.dat	2570	58831	6	102
flt020_ghostDance010_jan23.dat	1589	12266	4	60
flt030_solCanyon010_jan23.dat	5399	497	11	198
flttrace_br.dat	3216	27787	7	108
flttrace_gd.dat	2819	15319	6	97
flttrace_sc.dat	5980	24919	12	198
flttraces_3.dat	11267	7364	23	370
hrz010_n3ptn_jan23.dat	8755	33573	18	315
hrz020_tptwtsw1_jan23.dat	8643	29004	17	309
hrz030_tsw23_jan23.dat	8659	29540	17	313
hrz040_chn1n2_jan23.dat	8241	10617	17	299
hrz050_ppw_jan23.dat	9764	18379	20	354
hrz060_cfun_jan23.dat	9558	9594	19	341
hrz070_tcbw_jan23.dat	14713	57106	29	640
hrz080_cfmnn-1_jan23.dat	28326	61030	56	1232
repository_surface.dat	5882	8431	12	150
topo010.dat	1746037	24983	3411	60212
tunnel_axis.dat	5263	46901	11	98
waterelev_950912.dat	1008	45268	2	28
Grid Files				
flt010_bowRidge020.2grd	60483	25481	119	155
flt020_ghostDance020.2grd	60485	16814	119	180
flt030_solCanyon020.2grd	60484	14685	119	236
hrz010_n3ptn_1.2grd	10117	35488	20	35
hrz010_n3ptn_2.2grd	10119	12193	20	20
hrz010_n3ptn_3.2grd	10118	5309	20	24

Filename	Size(bytes)	Checksum	Blocks	Lines
hrz010_n3ptn_4.2grd	10118	58937	20	23
hrz020_tptwtsw1_1.2grd	10118	10623	20	22
hrz020_tptwtsw1_2.2grd	10120	56443	20	24
hrz020_tptwtsw1_3.2grd	10119	4068	20	15
hrz020_tptwtsw1_4.2grd	10119	48281	20	13
hrz030_tsw23_1.2grd	10109	35933	20	25
hrz030_tsw23_2.2grd	10111	20603	20	30
hrz030_tsw23_3.2grd	10110	26345	20	26
hrz030_tsw23_4.2grd	10110	527	20	20
hrz040_chn1n2_1.2grd	10112	43506	20	24
hrz040_chn1n2_2.2grd	10114	60017	20	27
hrz040_chn1n2_3.2grd	10113	13357	20	19
hrz040_chn1n2_4.2grd	10113	44763	20	27
hrz050_ppw_1.2grd	10103	49980	20	20
hrz050_ppw_2.2grd	10105	7674	20	33
hrz050_ppw_3.2grd	10104	30553	20	32
hrz050_ppw_4.2grd	10104	33482	20	23
hrz060_cfun_1.2grd	10106	30892	20	23
hrz060_cfun_2.2grd	10108	60380	20	40
hrz060_cfun_3.2grd	10107	26194	20	33
hrz060_cfun_4.2grd	10107	400	20	27
hrz070_tcbw_1.2grd	10106	17466	20	57
hrz070_tcbw_2.2grd	10108	54959	20	53
hrz070_tcbw_3.2grd	10107	13809	20	48
hrz070_tcbw_4.2grd	10107	30988	20	91
hrz080_cfmnn-1_1.2grd	10121	2704	20	43
hrz080_cfmnn-1_2.2grd	10123	14467	20	31
hrz080_cfmnn-1_3.2grd	10122	25972	20	35

Filename	Size(bytes)	Checksum	Blocks	Lines
hrz080_cfmnn-1_4.2grd	10122	41917	20	62
topo020.2grd	60466	2588	119	119
water.2grd	60475	6009	119	116
Polygon Files				
flt020_ghostDance030.ply	759	48733	2	35
repository.ply	3662	46298	8	151
Sequence Files				
s010_porosity.seq	5330	9644	11	309
s020_satcond.seq	5395	13161	11	309
Faces Files				
m01_porosity.faces	12032000	45873	23500	68212
m02_satcond.faces	12032000	13638	23500	68210
m03_photo.faces	18540544	60691	36212	117812
m04_landsat.faces	18540544	38328	36212	117554
topo030M_aerial.faces	6541312	6742	12776	49605
topo030M_landsat.faces	6541312	44464	12776	49347
Image Files				
aerialphoto1.rgb	2021469	52937	3949	1262
landsat.rgb	347072	36505	678	3
Image Registration Files				
aerialphoto1.imreg	87	4863	1	7
landsat.imreg	73	3843	1	7
Vue Files				
v01_map.vue	2950	34786	6	175
v02_bholes.vue	2956	35432	6	175
v03_zones.vue	2971	36637	6	173
v04_block.vue	3020	41318	6	175
v05_watertable.vue	2971	36633	6	173

Filename	Size(bytes)	Checksum	Blocks	Lines
v06_faults.vue	3134	48509	7	180
v07_porosity.vue	3097	47938	7	178
v08_repos.vue	3104	48217	7	178
v09_zcolor.vue	3092	47256	7	178
v10_satcond.vue	3095	47625	7	178
v11_photo.vue	2967	36303	6	173
v13_landsat.vue	2992	38542	6	174
v14_porholes.vue	3338	1318	7	191
v15_scholes.vue	3336	830	7	191
Color Table Files				
logsat.pclr	352	13761	1	23
porosity.pclr	352	13890	1	23
zones.zclr	1679	65526	4	65
zones.znclr	352	13428	1	23
Vertical Fault Files				
repository.vflt	3848	45430	8	141
tunnel.vflt	3026	16931	6	96
Annotation Files				
a01_map.ann	36540	36545	72	1809
a02_boreholes.ann	33291	27217	66	1648
a03_20bholes.ann	2044	59609	4	102
a04_empty.ann	1070	9508	3	55
a05_repository.ann	3278	42910	7	168
a06_esf.ann	2199	52594	5	113
a07_3dmodel.ann	613	43077	2	32
a08_5kmCircle.ann	2663	6056	6	98
a09_crossSections.ann	703	47232	2	36
a10_oneillflts.ann	221086	28659	432	6473

Filename	Size(bytes)	Checksum	Blocks	Lines
a11_porosity.ann	1426	24240	3	74
a12_satcond.ann	1501	28569	3	78
a13_8bholes.ann	1029	1642	3	54
a14_3faults.ann	4110	12822	9	206
a15_waterElev.ann	1590	35463	4	96
a31_3faults.ann	6328	54181	13	377
a51_area.ann	11080	35314	22	541
a61_area.ann	7830	18345	16	406
Script Files				
run010_mkFltGrds.sh	1840	47221	4	70
run020_mkHorzGrds.sh	2179	3827	5	66
run030_mkPorFaces.sh	771	1591	2	12
run040_mkSCFaces.sh	779	1695	2	12
run050_mkPhotoTopo.sh	239	14737	1	14
run060_mkPhotoFaces.sh	129	9928	1	7
run070_mkTmTopo.sh	235	14376	1	14
run080_mkTmFaces.sh	132	10239	1	7
Text Files				
t01_grids.txt	1491	51717	3	44
t02_list.txt	8921	62861	18	136
t03_ranges.txt	2536	1919	5	49
t04_topo_stats.txt	1220	63235	3	23
t05_water.txt	1863	20255	4	32

APPENDIX B

CATALOG OF BOREHOLE INFORMATION ON POROSITY, SATURATED HYDRAULIC CONDUCTIVITY, AND DEGREE OF WELDING OF LITHOSTRATIGRAPHIC UNITS USED IN CONSTRUCTION OF THE PRELIMINARY THREE-DIMENSIONAL HYDROSTRATIGRAPHIC MODELS

Legend

m	=	meters
m/s	=	meters per second

Degree of Welding

non	=	non-welded
part	=	partially welded
mod	=	moderately welded
dense	=	densely welded

Detailed porosity and saturated hydraulic conductivity data and information on degree of welding of lithostratigraphic units was determined from borehole logs in the USGS reports cited in the text (Sections 4.2.3. and 4.2.4). Lithostratigraphic unit designations in parentheses are those used in the 3D geological framework model.

Table B-1. Tiva Canyon (Tpcw)

TIVA CANYON (Tpcw)				
Depth (m)	Porosity	Hydraulic Conductivity (m/s)	Degree of Welding	Borehole ID
43	0.414	9.60E-07	non-part	UE25a#4
41	0.431	9.60E-11	non-part	UE25a#6
63	0.070	2.10E-10	mod-dense	USWG-3
78	0.075	7.90E-12	mod-dense	USWG-3
93	0.093	2.20E-11	mod-dense	USWG-3
18	0.057	4.60E-10	dense	USWG-4
28	0.081	2.15E-10	dense	USWG-4

Table B-2. Yucca Mountain (n3-PTn)

YUCCA MOUNTAIN (n3-PTn)				
Depth (m)	Porosity	Hydraulic Conductivity (m/s)	Degree of Welding	Borehole ID
47	0.418	2.30E-06	non	UE25a#4
48	0.444	1.90E-06	non	UE25a#4
51	0.420	1.60E-07	non	UE25a#6
34	0.450	—	non-part	USWH-1
34	0.430	—	non-part	USWH-1
42	0.320	2.60E-08	part	UE25UZ#5

Table B-3. Pah Canyon (n3-PTn)

PAH CANYON (n3-PTn)				
Depth (m)	**Porosity**	**Hydraulic Conductivity (m/s)**	**Degree of Welding**	**Borehole ID**
77	0.480	—	non	USWH-1
73	0.410	1.32E-08	part	UE25UZ#4
85	0.470	5.25E-07	part	UE25UZ#4
71	0.464	1.90E-07	part	UE25UZ#5
80	0.455	6.80E-09	part	UE25UZ#5

Table B-4. Topopah Spring (Tptw-TSw1 and TSw2+3)

TOPOPAH SPRING (Tptw-TSw1 and TSw2+3)				
Depth (m)	Porosity	Hydraulic Conductivity (m/s)	Degree of Welding	Borehole ID
226	0.118	1.40E-11	dense	UE25b#1
133	0.170	8.05E-09	mod	USWG-3
141	0.177	8.20E-09	mod	USWG-3
168	0.139	8.00E-11	mod	USWG-3
176	0.119	4.10E-11	mod	USWG-3
186	0.109	1.30E-11	mod	USWG-3
201	0.209	2.80E-09	mod	USWG-3
218	0.087	1.50E-11	mod-dense	USWG-3
233	0.131	6.80E-12	mod-dense	USWG-3
252	0.066	5.03E-13	mod-dense	USWG-3
270	0.107	7.70E-10	mod-dense	USWG-3
282	0.096	2.19E-11	mod-dense	USWG-3
292	0.087	6.35E-11	mod-dense	USWG-3
322	0.102	9.70E-14	mod-dense	USWG-3
338	0.088	1.72E-10	mod-dense	USWG-3
356	0.099	2.20E-10	mod-dense	USWG-3
370	0.026	3.52E-10	dense	USWG-3
385	0.030	5.50E-11	dense	USWG-3
400	0.273	6.80E-08	non	USWG-3
86	0.123	3.70E-09	mod-dense	USWG-4
101	0.167	1.80E-09	mod-dense	USWG-4
119	0.118	4.80E-10	mod-dense	USWG-4
167	0.117	6.30E-08	dense	USWG-4
184	0.168	2.20E-09	dense	USWG-4
204	0.148	3.87E-10	mod-dense	USWG-4
226	0.077	7.50E-10	dense	USWG-4

Table B-4. Topopah Spring (Tptw-TSw1 and TSw2+3) (Cont'd)

TOPOPAH SPRING (Tptw-TSw1 and TSw2+3)				
Depth (m)	Porosity	Hydraulic Conductivity (m/s)	Degree of Welding	Borehole ID
250	0.110	3.25E-11	dense	USWG-4
267	0.101	9.70E-14	dense	USWG-4
286	0.109	1.30E-11	dense	USWG-4
325	0.187	1.86E-09	dense	USWG-4
378	0.089	9.70E-14	dense	USWG-4
415	0.150	1.00E-10	part	USWG-4
128	0.220	—	mod-dense	USWH-1
129	0.240	—	mod-dense	USWH-1
135	0.210	—	mod-dense	USWH-1
137	0.190	—	mod-dense	USWH-1
140	0.160	—	mod-dense	USWH-1
141	0.170	—	mod-dense	USWH-1
142	0.170	—	mod-dense	USWH-1
143	0.150	—	mod-dense	USWH-1
219	0.170	—	mod-dense	USWH-1
221	0.280	—	mod-dense	USWH-1
222	0.180	—	mod-dense	USWH-1
226	—	—	mod-dense	USWH-1
390	0.160	—	mod-dense	USWH-1
391	0.160	—	mod-dense	USWH-1
398	0.140	—	mod-dense	USWH-1
399	0.100	—	mod-dense	USWH-1
405	0.120	—	mod-dense	USWH-1
406	0.110	—	mod-dense	USWH-1
106	0.287	160E-06	non	UE25UZ#5

Table B-5. Calico Hills (CHn1..3-n2)

CALICO HILLS (CHn1..3-n2)				
Depth (m)	**Porosity**	**Hydraulic Conductivity (m/s)**	**Degree of Welding**	**Borehole ID**
479	0.281	1.20E-09	non	UE25b#1
440	0.311	8.00E-11	non	USWG-1
488	0.233	2.20E-10	non	USWG-1
505	0.315	—	non	USWG-1
518	0.320	9.60E-11	non	USWG-1
536	0.290	9.60E-11	non	USWG-1
544	0.253	—	non	USWG-1
546	0.334	9.60E-11	non	USWG-1
457.9	0.357	2.95E-07	non	USWG-3
511.7	0.309	1.20E-10	non	USWG-4
531	0.470	—	non	USWH-1
533	0.440	—	non	USWH-1

Table B-6. Prow Pass (PPw)

PROW PASS (PPw)				
Depth (m)	**Porosity**	**Hydraulic Conductivity (m/s)**	**Degree of Welding**	**Borehole ID**
626	0.252	—	non-part	UE25b#1
680	0.136	—	part	UE25b#1
573	0.340	1.90E-10	part-mod	USWG-1
589	0.340	2.40E-10	part-mod	USWG-1
624	0.270	1.40E-10	part-mod	USWG-1
633	0.280	1.10E-10	part-mod	USWG-1
499.3	0.354	4.60E-07	part	USWG-3
508.1	0.317	8.95E-08	part	USWG-3
520.3	0.262	2.25E-08	part	USWG-3
552.9	0.387	1.50E-09	part	USWG-3
589.2	0.328	2.95E-10	part	USWG-3
583.1	0.325	1.10E-10	non-part	USWG-3
597.1	0.344	1.30E-10	non-part	USWG-3
555.7	0.342	5.65E-08	part	USWG-4
570.3	0.292	3.25E-08	part	USWG-4
584.1	0.19	—	part	USWG-4
640.0	0.33	9.80E-10	part	USWH-1
641.0	0.32	6.70E-10	part	USWH-1

Table B-7. Crater Flat Upper nonwelded (CFUn)

CRATER FLAT UPPER NONWELDED (CFUn)				
Depth (m)	**Porosity**	**Hydraulic Conductivity (m/s)**	**Degree of Welding**	**Borehole ID**
661	0.260	3.85E-11	non	USWG-1
602.4	0.326	8.35E-10	non-part	USWG-4
619.6	0.316	4.70E-10	part	USWG-4
649.8	0.242	4.30E-10	part	USWG-4
665.2	02.71	1.14E-10	part	USWG-4
679.4	0.316	2.98E-09	non	USWG-4

Table B-8. Bullfrog (BFw)

BULLFROG (BFw)				
Depth (m)	Porosity	Hydraulic Conductivity (m/s)	Degree of Welding	Borehole ID
753	0.233	—	part	UE25b#1
789	0.216	—	part	UE25b#1
814	0.221	—	mod	UE25b#1
844	0.227	—	mod	UE25b#1
612.3	0.325	6.10E-10	part	USWG-3
632.6	0.299	1.10E-07	part	USWG-3
643.3	0.135	1.10E-09	mod	USWG-3
660.8	0.18	2.00E-09	mod	USWG-3
672.2	0.09	—	mod	USWG-3
688	0.085	4.95E-12	mod	USWG-3
705.8	0.08	3.90E-12	mod	USWG-3
718.5	0.071	2.45E-11	mod	USWG-3
733.9	0.072	5.55E-12	mod-dense	USWG-3
752.6	0.055	6.80E-12	mod-dense	USWG-3
768.8	0.106	5.95E-11	mod	USWG-3
781.2	0.319	3.80E-09	part	USWG-3
700.6	0.256	1.80E-08	part	USWG-4
712.4	0.262	2.60E-08	part	USWG-4
726.1	0.209	4.05E-09	mod	USWG-4
742.7	0.252	3.95E-08	part	USWG-4
755.5	0.253	6.25E-08	part	USWG-4
769.4	0.234	2.55E-08	part	USWG-4
785.9	0.186	9.10E-10	part	USWG-4
804.1	0.107	7.40E-11	part	USWG-4
821.5	0.239	4.50E-10	part	USWG-4
829.1	0.227	3.80E-08	mod-dense	USWG-4

Table B-8. Bullfrog (BFw) (Cont'd)

BULLFROG (BFw)				
Depth (m)	Porosity	Hydraulic Conductivity (m/s)	Degree of Welding	Borehole ID
709.0	0.33	1.60E-09	non-mod	USWH-1
710.0	0.38	6.95E-09	non-mod	USWH-1
713.0	0.19	8.30E-10	non-mod	USWH-1
764.0	0.28	7.75E-09	non-mod	USWH-1
772.0	0.25	4.60E-09	non-mod	USWH-1
790.0	0.19	4.60E-10	non-mod	USWH-1
791.0	0.19	8.10E-10	non-mod	USWH-1
792.0	0.21	5.80E-10	non-mod	USWH-1
830.0	0.27	4.05E-10	non-mod	USWH-1